

Department of Medical Biology

An investigation of Intercellular Adhesion Molecule-1 (ICAM-1) in Breast Cancer

Bryan George Vincent Elston

Master thesis in Biomedicine [MBI-3911] May 2016



Acknowledgements

This work was performed at the RNA and Molecular Pathology (RAMP) group, Department of Medical Biology (IMB), Faculty of Health Science at the University of Tromsø from August 2015 to May 2016.

I would like to thank my supervisor, Kristin Fenton, for her excellent support and guidance through the practical work, analysis and thesis writing.

I would like to thank Stine Figenschau for her guidance and help with performing and understanding the experiments in the laboratory.

Thanks to Prema Kanapathippillai for her knowledge and skill in the laboratory and helpful attitude.

Thank you to my fellow Masters students – Mike Ampong, Ibrahim Abdulsalam and Betty Furulund for fun and enjoyable times.

Finally, a great big thankyou to my family for all their help and love, especially Tonje my supportive wife, and my father who came to stay and help us during a busy time.

Bryan Elston

Tromsø, May 2016.

Summary

Intercellular Adhesion Molecule-1 (ICAM-1, CD54), a cell surface glycoprotein that functions as an integrin, has a well-established role in leukocyte migration during inflammation. Recent studies have indicated a role for this protein in cancer development. In this study three breast cancer cell lines were stimulated with a variety of cytokines. The breast cancer cell lines (MCF7, SK-BR-3 and MDA-MB-468) were chosen to reflect the hormone positive, HER-2 enriched and triple negative subtypes of breast cancer. The cytokines (Interferon gamma, Tumour Necrosis Factor alpha, Interleukin 1beta and Interferon alpha) are commonly encountered in the breast cancer micro-environment. Relative gene expression was measured using quantitative real time polymerase chain reaction. ICAM-1 protein was measured by Western Blot and localised by Immunofluorescence. In addition, ICAM-1 gene expression was measured in human breast cancer samples and ICAM-1 and macrophage (CD68) immunohistochemistry was performed on formalin-fixed, paraffin embedded tumour tissue.

ICAM-1 expression was induced in all of the cell lines by $\text{IFN}\gamma$, $\text{TNF}\alpha$ and $\text{IL-1}\beta$ with increased ICAM-1 protein production compared to time-matched controls. $\text{IFN}\alpha$ appeared to induce ICAM-1 gene expression but no protein was detected. Membranous and para-nuclear ICAM-1 staining was identified after 24 hours in unstimulated MCF7 and MDA-MB-468 cells and the same cell lines stimulated with $\text{IFN}\gamma$. ICAM-1 expression was increased in the human tumour tissue compared to normal tissue. However, this did not correspond with ICAM-1 positivity or numbers of macrophages in the tumour.

The study highlights a mechanism that cancer cells may use to enhance their invasive and metastatic potential by making use of a protein normally involved in cell migration.

Abbreviations

ATCC	-	American Type Culture Collection
cDNA	-	Complementary Deoxyribonucleic Acid
DMEM	-	Dulbecco's Modified Eagles Medium
DMSO	-	Dimethyl sulfoxide
ELISA	-	Enzyme-Linked Immunosorbent Assay
EMT	-	Epithelial Mesenchymal Transition
ER	-	Oestrogen Receptor
FAM	-	Fluorochrome, 6-carboxyfluorescein
FFPE	-	Formalin Fixed, Paraffin Embedded
HER-2	-	Human Epidermal Growth Factor Receptor-2
IFN α	-	Interferon alpha
IFN γ	-	Interferon gamma
IL-1 β	-	Interleukin-1beta
LDS	-	Lithium dodecyl sulphate
MUC1	-	Mucin 1, cell surface associated
mRNA	-	Messenger RNA
NaOH	-	Sodium Hydroxide
PBS	-	Phosphate Buffered Saline
PCR	-	Polymerase Chain Reaction
PMN	-	Polymorphonuclear leukocyte
PVDF	-	Polyvinylidene Difluoride
PR	-	Progesterone Receptor
qPCR	-	Quantitative Real Time Polymerase Chain Reaction

RNase	-	Ribonuclease
RNA	-	Ribonucleic acid
RPM	-	Rotations per minute
RPMI	-	Roswell Park Memorial Institute Medium
sICAM1	-	Soluble Intercellular Adhesion Molecule-1
TBST	-	Tris-buffered Saline with Tween 20
TNF α	-	Tumour Necrosis Factor alpha

1. Introduction

1.1. Breast cancer

Breast cancer is one of the most common invasive cancers affecting women and one of the most common causes of cancer deaths world-wide. In 2013, 3,220 women and 36 men were diagnosed with breast cancer in Norway [1]. Understanding of the molecular changes has informed a classification system that reflects disease prognosis and therapeutic options [2].

1.1.1 Breast Cancer classification

Breast cancer is a heterogeneous group of neoplasms originating from the epithelial cells lining the milk ducts [3]. The diversity between the tumours and the individuals harbouring these tumours combine to determine the risk of disease progression and therapeutic resistance. Making distinctions about different types of breast cancer is useful as it can reflect a differing natural history for each sub-type of breast cancer [2].

Relatively recently, molecular classification has become increasingly implemented in categorizing breast cancer [4]. This work has led to the concept of six general subtypes of breast cancer: Luminal A, Luminal B, human epidermal growth factor receptor 2 (HER2)-enriched, basal-like, claudin-low and normal breast-like [5].

The luminal subtype shows gene expression similar to normal breast duct epithelia and includes transcriptional factors such as GATA3 and FOXA1 known to be important for luminal differentiation [6]. The luminal subtype often expresses estrogen receptor (ER), progesterone receptor (PR) and HER2. This subtype is divided into two subclasses – luminal A and luminal B [7]. The luminal A subtype is HER2 negative with a high expression of ER and PR and an overall low proliferation rate. Luminal B tumours

express high levels of ER and PR and are either HER2 positive or HER2 negative with a high proliferative rate [8]. The gene expression of the basal-like subtype resembles normal basal/myoepithelial cells of the breast and frequently lack ER, PR and HER2 overexpression. They also show mutations in the tumour suppressor gene p53 (TP53) and have high proliferation rates. Gene expression profiling show the basal-like subtype to be associated with a poor prognosis [9].

The majority of the basal-like subtype of breast cancers are ER, PR and HER2 negative. Basal-like cancer is an entity defined using gene expression analysis whereas ER, PR and HER-2 negative (triple-negative) breast cancer is a phenotype based on immunohistochemistry and, although there are many similarities, they are not synonymous [10].

The HER2 enriched subgroup has a low expression of ER and genes associated with oestrogen metabolism. HER2 overexpression is usually caused by gene amplification driving genomic instability in chromosome 17q and overexpression of other genes in this region [5]. 10-20% of breast cancers are HER2 enriched and the prognosis is poor compared to luminal subtypes, frequently complicated by brain metastases. It is an aggressive subtype with a higher risk of both local and regional relapse [11]. The HER2 tyrosine kinase receptors trigger a complex array of signalling pathways that regulate normal cell growth and promote tumorigenesis, cell proliferation, cell survival, migration, differentiation and angiogenesis [12].

Claudin-low tumours are similar to HER2-enriched and basal-like tumours in prognosis and are differentiated by a mesenchymal phenotype reflected in their expression of vimentin and N-cadherin [13]. These tumours that show enrichment in epithelial-mesenchymal transition (EMT) and stem cell-like features while showing a low expression of luminal and proliferation associated genes [14].

The normal-like breast cancer has a high expression of genes characteristic for basal epithelial cells and adipose cells and a low expression of the genes expressed in luminal

epithelial cells. It has been proposed to be an artefact of tumour specimen contamination by normal tissue [15].

1.1.2. Breast cancer cell lines

Breast cancer cell lines are the most widely used model system to investigate the deregulation of proliferation, apoptosis and migration in breast cancer [16]. Cell lines are easily propagated and yield reproducible results when used with well-defined experimental conditions [17]. Human cells may have more relevance to human disease compared to animal models and there is uncertainty about whether the same genetic alterations transform both mouse and human epithelial cells [18].

Three main subtypes of breast cancer cell lines are identified by gene expression, Luminal, Basal A and Basal B [19, 20]. The luminal subtype contains ER positive cell lines with good prognostic signatures. The basal A subtype contains ER negative cell lines which resemble basal-like tumours and are associated with early onset hereditary breast cancer genes (BRCA1). The basal B subtype is characterised by markers that are associated with more aggressive tumours including mesenchymal and stem cell characteristics with up regulation of epidermal growth factor (EGF)[17].

The majority of the luminal cell lines are similar to the luminal A or luminal B tumours, the basal-A show similarities with the basal-like tumours and the basal B cell line is compatible with the basal-like or the HER-2 enriched tumours [21].

There is some discrepancy between subtypes of primary tumours and cell lines due to the presence of normal epithelial and stromal cells in the primary tumour samples and the absence of stromal, tumour and inflammatory interactions in cell culture. It has been shown that differences between the genome aberration patterns for the basal like and luminal clusters in the cell lines do not always reflect the differences in these

subtypes in primary tumours, suggesting that the cell lines may be derived from subpopulations of tumours cells that are selected because they grow well in culture [22].

Comparisons between cell lines and primary tumours have shown that cell lines mirror both the genomic heterogeneity and the recurrent genome copy number abnormalities found in primary tumours [20]. Breast cancer cell lines are seen as an appropriate model system for investigating the functional consequences of gene deregulation, identification of molecular features of breast cancer and biomarker discovery [23].

1.2. Inflammatory milieu in breast cancer

Cancers arise in a microenvironment containing elements normally seen in chronic inflammation, including cells (macrophages, lymphocytes, dendritic cells) and soluble messengers (cytokines). It appears that dysregulation of the pathways that would normally lead to resolution of the inflammation instead promote proliferation, mutation and neoplastic transformation [24]. Interferon gamma, Tumour Necrosis Factor alpha, Interleukin-1beta and Interferon alpha are examples of cytokines that occur in this inflammatory microenvironment [25].

1.2.1. Interferon gamma (IFN γ)

Interferon gamma is involved in multiple functions including prevention of viral replication, modulation of cell differentiation and inhibition of cell growth through interactions with its two receptors, IFN γ -R α and IFN γ -R β [26]. It is considered to have anti-tumour effects and has been shown to cause growth arrest in breast cancer cell lines [27]. However it may also be able to drive chronic inflammation and affect immune-editing in a way that promotes cancer [28].

1.2.2. Tumour Necrosis Factor alpha (TNF α)

Tumour Necrosis Factor alpha is a proinflammatory cytokine produced by macrophages, monocytes, T-lymphocytes and mast cells. It binds to the tumour necrosis factor receptors type I and II to mediate its biological effects, including the stimulation of pro-inflammatory genes and either cell survival or apoptosis. There is evidence that TNF α can cause tumour cell death and regression but over-expression of TNF α can lead to chronic inflammation and cancer formation [29].

1.2.3. Interleukin-1beta (IL-1 β)

IL-1 β is a pro-inflammatory cytokine produced by macrophages, T and B lymphocytes, natural killer (NK) cells and neutrophils. It is part of the interleukin-1 cytokine superfamily with interleukin-1 alpha (IL-1 α) and interleukin receptor antagonist [30]. It is involved in cell proliferation, differentiation and apoptosis. High levels in breast cancer specimens have been noted to correlate with aggressive disease [31].

1.2.4. Interferon alpha (IFN α)

IFN α is a type I interferon and acts at a different receptor to IFN γ . It is produced by many cell types (including macrophages, T and B lymphocytes, endothelial cells and fibroblasts) to activate macrophages, dendritic cells and NK cells to evoke antiviral and anti-neoplastic effects [32]. It has been used to treat haematological cancers in humans [33] and to enhance immune-mediated clearance of human breast cancer cells transplanted into a mice model [34].

1.3. Intercellular Adhesion Molecule 1 (ICAM-1)

Intercellular Adhesion Molecule-1 (ICAM-1), or CD54, is a member of the immunoglobulin superfamily and is a cell surface glycoprotein that is expressed on normal vascular endothelial cells, peripheral lymphoid tissue and some parenchymal cells [35]. It is involved in cell-cell and cell-matrix adhesion and much research has been performed on its role in inflammation [36]. It has been shown to be induced by several cytokines in its role as an adherence molecule [35]. A soluble form is also identified in the blood and is presumed to be a surface protein that has been shed by cells [37].

Recent studies indicate a possible role in cancer development. Stomach epithelium does not display immunoreactivity for ICAM-1, however gastric cancer is positive for ICAM-1 immunohistochemistry with accentuation at the invading front of the tumour. High levels of soluble ICAM-1 (sICAM-1), believed to be shed from the gastric cancer, correlate with lymph node metastasis and poor prognosis [38].

Melanoma prognosis is strongly associated with depth of invasion [39]. Melanomas less than 0.75 mm in thickness do not express significant amounts of ICAM-1 and those greater than 1mm in thickness express ICAM-1 strongly. The thicker tumour has an increased risk of metastasis [40].

Colon cancer similarly shows an association between nodal metastases and circulating sICAM-1[41]. Immunostaining of colorectal cancers show increased ICAM-1 staining, particularly in cells that lie close to blood vessels[42].

Concerning breast cancer, ICAM-1 expression is absent in normal breast tissue but can be seen in tumours [43]. Assays of sICAM-1 in the blood show a significant increase occurring with increased stage of breast cancer [44]. The site of several ICAM genes on chromosome 19 was identified as a possible breast cancer susceptibility locus and the level of expression of ICAM-1 on the cell surface was found to correlate with the

metastatic potential of several breast cancer cell lines, while downregulation of mRNA and protein expression decreased invasion of cells through a matrigel matrix [45]. Recently overexpression of ICAM-1 has been described in triple negative breast cancers and proposed as a possible target for therapy [46].

A hypothesis has been proposed by Roland *et al* describing a mechanism by which ICAM-1 may be involved in carcinogenesis [47]. This hypothesis is that circulating tumour cells bind to endothelial ICAM-1 via tumour expressed cell surface Mucin-1 (MUC-1) resulting in release of cytokines and chemokines by the tumour cell. These soluble mediators attract macrophages and upregulate ICAM-1 in tumour cells and endothelial cells. This leads to an expanding mass of tumour cells and tumour associated macrophages (TAMs) that may further attract neutrophils (PMNs) to release elastases to break down extracellular barriers to cell migration.

2. Aim of Study

The aim of the project was to examine the expression of the ICAM-1 gene in representative breast cancer cell lines and test whether the gene and its product could be induced by inflammatory cytokines commonly present in the tumour micro-environment. A further aim was to compare the breast cancer cell line results to ICAM-1 expression in a cohort of human tumour samples.

3. Materials and Methods

3.1. Breast cancer cell lines

The MDA-MB-468, SK-BR-3 and MCF-7 breast cancer cell lines were used in this study (Table 3.1).

MDA-MB-468 is a Basal-B breast cancer cell line and does not have progesterone receptor (PR), estrogen receptor (ER) or the Her2 receptor (human epidermal growth factor 2). The cell line was isolated from a pleural effusion of a 51-year-old black female. It expresses epidermal growth factor receptor (EGFR) and transforming growth factor alpha receptor (TGF alpha) [13].

SK-BR-3 is a luminal breast cancer cell line that over-expresses the HER2-gene product but is negative for ER and PR. It has a high proliferation rate as measured by Ki67 immunohistochemistry and has been used to research anti-HER-2 antibody treatment [48]. The founding cells were isolated from a pleural effusion in a 43-year-old Caucasian female.

MCF-7 is a luminal breast cancer cell line that expresses progesterone receptor (PR) and estrogen receptor (ER). The cell line was isolated from the pleural effusion of a 67-year-old Caucasian female [49]. The cell line expresses the WNT7B oncogene and retain some characteristics of differentiated mammary epithelial cells, such as forming domes and process oestradiol via cytoplasmic estrogen receptors. The growth of the cell line is inhibited by tumour necrosis factor alpha (TNF α) [20].

Table 3.1. Breast cancer cell line with relevant subclass, hormonal status and HER-2 enrichment. [19, 20, 22]

Breast cancer cell line	Subclass	ER/PR/HER2 status
MCF7	Luminal	ER+/PR+/HER2-
SK-BR-3	Luminal	ER-/PR-/HER2+
MDA-MB-468	Basal A	ER-/PR-/HER2-

3.2. Cell line stimulation

Each cell line was grown and sub-cultured according to ATCC guidelines. MCF7 was grown in Dulbecco's Modified Eagle's Medium (DMEM) with 10% Fetal Bovine Serum (FBS), 1% glutamine, 1% penicillin and streptomycin and 0.01 mg/ml insulin. MDA-MB-468 and SK-BR-3 cells were grown in Roswell Park Institute Medium (RPMI) with 10% FBS, 1% glutamine and 1% penicillin and streptomycin. The cells were cultured to confluency in a 175 cm² culture flask and plated into 6 well plates, 1x10⁵ cells per well. The cells were allowed to grow in the plate for 6-12 hours before the medium was changed to a starvation medium with only 5% FBS. After a further 12 hours conditioning in the starvation medium, the cells were stimulated with one of the following cytokines: IFN γ (50ng/ml), TNF α (5ng/ml), Il1 β (25ng/ml) and IFN α (16 ng/ml). Plates were harvested at 0, 3, 6, 12, 24 and 48 hours. Separate plates at each time point were made for RNA and protein isolation with appropriate non-stimulated controls. RNA isolates were made with three replicates. At harvest, the cell culture medium was removed while the plates were kept on ice. The medium was stored at -80C but not used in this project. The wells were then washed twice with 1ml PBS and then 1ml Trizol-reagent added for RNA isolation or 100 μ l NuPAGE LDS Sample Buffer added for protein isolation as detailed below.

3.3. RNA isolation

Total RNA was isolated from the stimulated cell lines by the following protocol:

- a. Cell lysis: The cells were lysed by adding 1 ml of Trizol-reagent (Sigma-Aldrich) to each well. The solution was pipetted several times to aid in disruption of cell membranes. The Trizol-reagent is a one-phase solution that contains Phenol and Guanidine Isothiocyanate that deactivates RNases, lyses cells and stabilizes RNA [50]. The solution was transferred to 1.5ml DNA LoBind Eppendorf tubes and incubated at room temperature for 5 minutes completing nucleoprotein complex dissociation. The samples were frozen at -80C.
- b. Phase separation: After thawing of the samples, 0.2 volumes of chloroform to Trizol were added and the tubes were left on ice for 20 minutes with shaking every second minute. The resulting mixture was centrifuged for 30 minutes at 4C and 9000 rpm. After centrifugation the sample separated into an upper aqueous phase, an interphase and a lower phenol-chloroform phase. The majority of the aqueous phase was removed and transferred to a new 1.5ml DNA LoBind Eppendorf tube. Care was taken not to disturb the interphase during this step (to avoid contaminating the RNA sample with DNA). The majority of the lower organic phase was removed from the original tube, a further 5-minute centrifugation at 9000 rpm and 4C was performed and a portion of the resulting aqueous phase transferred to the new tube.
- c. RNA precipitation: An equal volume of isopropanol was added to the newly separated aqueous phase, the sample was mixed well and incubated overnight at -20C. Following this, the samples were centrifuged for 30 minutes at 15000rpm and 4C. The supernatant was decanted.
- d. RNA wash: 1ml of ice cold 80% Ethanol was added to the Eppendorf tube and the specimen centrifuged at 15000g for 5 minutes at 4C. The ethanol was removed and the specimens centrifuged again at 15000g for 1 minute at room temperature. After removing the remaining ethanol, the pellet was air-dried for 10-20 minutes

- e. RNA re-suspension: The dried pellet was dissolved in 10 μ l nuclease free water by pipetting the sample multiple times.

Another source of RNA was used in this project for determination of ICAM-1 gene expression levels in human breast tissue (Table A1). This tissue was collected from 23 patients undergoing breast cancer surgery and 2 patients undergoing breast surgery for non-cancerous disease. RNA isolation and deep sequencing were performed to this project. Some of the stored RNA was used for real-time PCR analysis of ICAM-1 expression. The RNA isolated from the breast cancer patients had matched RNA isolated from macroscopically normal appearing breast tissue in the same operative specimen, these samples are termed 'N' in the remainder of the thesis. RNA from the two operative specimens not containing cancerous tissue is termed 'NN' in the rest of the thesis.

3.4. RNA measurement

Both the Qubit Fluorometer (Invitrogen/Life Technologies) and the Nanodrop Spectrophotometer (ND 4000, Thermo Fisher Scientific) were used to quantify the amount of RNA present. The Qubit Fluorometer utilises proprietary dyes that emit fluorescent signals when bound to specific target molecules. The Nanodrop quantifies nucleic acid concentration by determining the absorption of ultraviolet light at 260nm and application of the Beer-Lambert law [51]. A higher absorbance at this wavelength correlates with a higher concentration of nucleic acid. The purity of nucleic acids is assessed in relation to proteins and organic compounds. The 260/280 ratio is used to assess protein contamination as 280nm is the peak absorbance wavelength for proteins. The 260/230 ratio is used to assess contamination by organic compounds as 230nm is the peak absorbance for organic compounds. Pure RNA should have a ratio of about 2 for both with lower values seen in the setting of contamination [51].

3.5. Protein isolation

100µl of NuPAGE LDS sampling buffer mixture was added to each well before scraping with a rubber policeman and transferring the samples to Eppendorf tubes. The samples were then denatured at 70°C for 10 minutes and store at -80C until further processing. The LDS, or lithium dodecyl sulphate is an anionic detergent that disrupts secondary and tertiary protein structures and adds negative electrical charges to proteins. The buffer mixture contains glycerol to help the samples sink into the gel wells and a reducing agent to keep the samples in a reduced state after heating [52]. The protein concentration was not measured in this project, actin (rabbit anti-actin antibody, Sigma Aldrich, product number A2066, lot number 090M4758) was chosen as a housekeeping protein to check the loading dose and normalise the Western blot results.

3.6. Western blotting

After thawing, the specimens were briefly sonicated before loading on NuPAGE Novex Bis-Tris Mini Gels with 15 wells. 15µl of each sample was loaded into lanes 2 to 14. 3µl SeeBlue pre-stained protein standard and 1.5µl MagicMark protein standard was loaded into lane 1 and a further 1.5µl MagicMark protein standard was loaded into lane 15. The gel was loaded into the XCell *Surelock*TM Mini-Cell system (Invitrogen) with 200ml running buffer and 500µl NuPAGE Antioxidant in the inner chamber and 600ml running buffer in the outer chamber. The system was then run at 200V for 35 minutes to separate the proteins.

The proteins were then transferred from the gel to a membrane in the XCell II Blot module (Invitrogen). The PVDF (Immobilon-P, Millipore) membrane was prepared by wetting it for 15 seconds in methanol and then transferring to deionised water for 2 minutes before placing it into 1XNuPAGE Transfer buffer for several minutes. Filter paper and blotting pads soaked in the same buffer were also used to prepare a gel-

membrane sandwich in the XCell II Blot module, which was run for 1 hour at a constant 30 volts. Only one gel was transferred per module in this project.

After transfer, the membrane was washed in Tris-buffered saline with 0.1% Tween (TBST) for 5 minutes and placed in a 50ml centrifuge tube with 3ml blocking solution for 1 hour. The membrane was then incubated overnight at 4°C with the primary antibody, anti-ICAM-1 (Abcam ab53013 [EP1aa2Y]) at a 1:2000 dilution. After overnight incubation, the membrane was washed in TBST 3 times, each wash for five minutes. Then the membrane was incubated with the secondary antibody, HRP goat anti-rabbit IgG heavy and light chain (Invitrogen product # 65-6120, lot 65-6120), for one hour at room temperature. The membrane was again washed 3 times in TBST, each wash lasting 5 minutes and then incubated with the SuperSignal West Pico Chemiluminescent Substrate (Pearce) for 5 minutes. The ImageQuant LAS 4000 (General Electric) was used to image the membrane using one-minute interval exposures. The membrane was then stripped with 0.5 M NaOH for 5 minutes before further washing in TBST (3x5 minutes), blocking for one hour at room temperature, incubation with rabbit anti-actin antibody (Sigma Aldrich, product number A2066, lot number 090M4758) and repeating of the previous steps to check for equal loading of the samples.

3.7. Immunohistochemistry for ICAM-1

Formalin fixed paraffin embedded (FFPE) tissue from a patient sample cohort that previously underwent deep-sequencing analysis and immunohistochemistry testing was used for immunohistochemistry with an anti-ICAM-1 antibody. Earlier microtome cut 4µm sections were placed in a rack in a 60°C heating cabinet overnight. The slides were deparaffinised through xylene (10 minutes) and graded alcohols (2 minutes each) to deionised water (2 minutes). Antigen retrieval was accomplished through immersing the sections in Citrate buffer (10mM Sodium Citrate, pH 6) within a DAKO PT-Link Pre Treatment Module preheated to 65°C and reaching a peak of 97°C for 20 minutes and returning to 65°C. The remaining steps were performed at room temperature.

The sections were transferred to PBS buffer before a blocking step for endogenous peroxidases with 200µl 3% H₂O₂ for 10 minutes. This was followed by 3 washes in PBS

for 3 minutes each. The next step was blocking non-specific hydrophobic binding by applying 200µl 10% goat serum diluted in PBS to the sections for 30 minutes. This was followed by 200µl of the primary antibody ICAM-1 (Abcam ab53013 [EP1aa2Y]) at a 1:50 dilution in 10% goat serum in PBS. Next three washes of three minutes each in PBS was performed.

The DAKO Envision+ System HRP (DAB) was used for visualisation of the primary antibody. The sections were incubated with 200µl Labelled Polymer Anti-Rabbit for 30 minutes. This was followed by three washes of PBS for three minutes each. The remaining steps were performed in a fume cabinet. The substrate-chromagen solution was prepared by mixing 20µl of Liquid DAB+ Chromogen per 1ml of Substrate Buffer. Sections were incubated with 200µl of this prepared substrate-chromagen solution for 10 minutes. They were then rinsed with deionised water. Counterstaining was performed with a 30 second period of immersion in haematoxylin followed by rinsing with deionised water until extinction of the red colour occurred. A 25 second period of immersion in Scott's solution was followed by a 2-minute wash in running deionised water. Sections were dehydrated through graded alcohols to xylene and cover-slipped with Histokit (Carl Roth).

The slides were examined by transmitted light microscopy with an Olympus BX51 microscope, attached camera and Cell imaging programme (Olympus Microscopy).

3.8. Immunohistochemistry for CD68

As part of the project slides that had previously been stained for macrophages with an anti-CD68 antibody were examined with the same microscope system. The sections containing tumour were assessed by a single operator initially in a semi-quantitative manner from 0 to +++ (0 = no CD68 positive cells in and around tumour, + = few CD68 positive cells, ++ = a moderate number of CD68-positive cells and +++ = a large number of CD68-positive cells).

3.9. Immunofluorescence for ICAM-1

Cells from the three cell lines were plated into 8 well slides with removable gaskets at a seeding density of 20,000 cells (in 200 μ l complete growth medium) per well. The cells were allowed to grow for 6 to 12 hours before the seeding medium was changed to starvation medium containing half the amount of FBS present in the complete growth medium. After a further 12 hours the cells were stimulated with IFN γ (2 wells), TNF α (2 wells) and IL1 β (2 wells). Two further wells were not stimulated. The slides were left to incubate for 24 hours before harvesting. CellTracker™ Green CMFDA (Invitrogen) was dissolved in dimethyl sulfoxide (DMSO) to a concentration of 2mg/ml and diluted in serum-free media to give a final concentration of 1 μ g/ml. After removing the stimulant and control media from the gasket wells, warmed CellTracker™ Green containing, serum-free media was added and the cells were incubated for 30 minutes at 37°C and 5%CO $_2$. After this time the dye working solution was replaced with fresh, pre-warmed medium and the cells were incubated for a further 30 minutes at the same growth conditions. The medium was then removed and the cells were washed 3 times for five minutes with PBS. The cells were fixed with 4% formaldehyde containing 0.1% Triton for 10 minutes at room temperature. Three further washes of five minutes each followed before the cells were incubated with 10% goat serum in PBS for 20 minutes at room temperature. Without washing the cells, the primary antibody (rabbit anti-ICAM-1) was added at 1:100 dilutions in 10% goat serum in PBS. Rabbit anti-vimentin (1:20) was used for the positive control. The cells were washed with PBS 3 times for five minutes each and the second antibody, goat anti-rabbit Alexa 546 Fab (1:500 dilution) in 10% goat serum in PBS. The cells were washed 3 times for 5 minutes each before placing the entire slide in methanol for 2 minutes and removing the gasket with a proprietary removal device. 5-10 μ l of DAPI were added per well, cover slips added and the edges sealed with nail polish. The slides were kept at 4°C until viewing with an Olympus X51 fluorescent microscope with appropriate filters, camera and imaging by the Cell imaging programme (Olympus microscopy).

3.10. cDNA synthesis

In order to synthesise a complementary DNA strand from RNA, the High Capacity cDNA Reverse Transcription kit (Life Technologies, catalogue no. 4368813) was used. The kit contains reverse transcriptase, reverse transcriptase buffers, deoxy-nucleotide triphosphates and random primers. For the breast cancer cell lines, RNA solution was diluted to 0.025µg/ml in a volume of 10µl Nuclease-free H₂O. A 10µl mixture of the Reverse Transcription kit was added to the diluted RNA sample. The mixture contained 2µl 10x RT buffer, 2µl 10x RT Random Primers, 0.8µl 25x dNTP Mix (100mM), 1ml Multiscribe Reverse Transcriptase and 4.2µl Nuclease-free H₂O. One control lacking template and another lacking the reverse transcriptase enzyme were prepared with each assay. The samples were briefly centrifuged and stored on ice until loading into a thermal cycler, programmed as per Table 3.2. The resulting cDNA was stored at -20°C.

Table 3.2. Settings for Thermal Cycler used for reverse transcription

	Step 1	Step 2	Step 3	Step 4
Temperature (°C)	25	37	85	4
Time	10 min	120 min	5 min	∞

3.11. Gene expression analysis

Quantitative real-time Polymerase Chain Reaction (qPCR) is a method for accurately quantifying the amount of a specified DNA sequence in a sample. Traditionally, the amount of PCR product is quantified at the end of the total amplification time. With qPCR, the PCR product is measured after each round of amplification. The reaction utilised Taq polymerase, isolated from the thermophile bacteria species *Thermus aquaticus*. It is a thermostable DNA polymerase that allows the PCR reaction by extending complimentary DNA strands from a primer while resisting the high

temperature (greater than 60°C) needed to denature the newly formed DNA strands and allow them to act as templates for the next round of amplification [53].

The quantification of the PCR product utilises a fluorescent label. The 5' end of the primer/probe is labelled with a reporter fluorochrome, 6-carboxyfluorescein (FAM). At the 3' end there is a quencher. The quencher absorbs the fluorescence of the reporter dye and no fluorescence is recorded. Taq polymerase has a 5'-3' nuclease activity that will cleave the probe during primer extension. The fluorophore is released from the effect of the quencher (due to increased intermolecular distance) and the amount of fluorescence released is recorded, being proportional to the PCR product generated in each cycle [53].

The cDNA samples and primer/probes were kept on ice at all times. As the primer/probes are sensitive to light, they were kept covered by aluminium foil. The Taqman® Fast Universal PCR Master Mix 2x (4352042, Applied Biosystems) was vortexed and briefly centrifuged prior to use. A master mix for each primer/probe was made with reference to the number of reactions to be performed (5µl Universal Master Mix, 0.5µl primer/probe mix, 2µl nuclease-free H₂O). The primer/probes used were ICAM-1 (Hs00164932, Applied Biosystems), RPLPO (Hs99999902, Applied Biosystems) and TBP (HS00427621_m1). A 96 well plate was placed on a plate-rack on ice and 7.5µl of the master mix and 2.5µl of cDNA was added to each well. Samples without template and controls from cDNA synthesis were included. The 96 well plate was covered with an optical adhesive cover and aluminium foil and stored on ice or a refrigerator until analysis. The plate was centrifuged at 1080g for 60 seconds to spin down contents and avoid bubbles before loading into a LightCycler 96 machine (Roche Diagnostics) for analysis with program as per Table 3.3.

Table 3.3. Programme for LightCycler 96 qPCR machine

Steps		Temperature	Time (seconds)
Preincubation		95°C	600
2 step amplification (40 cycles)	Step 1	95°C	15
	Step 2	60°C	60
Cooling		37°C	30

3.12. Statistics

Fold change was calculated by subtracting the mean threshold cycle number (Cq mean) of the housekeeping gene from the gene of interest. This number was corrected for the average of the unstimulated cultured cells at each time point and only the zero time-point. The fold change was then calculated by: $2^{-\Delta\Delta Cq}$. Data are shown as mean \pm SEM. Statistical significance was assessed using a Mann-Whitney U test, One-way ANOVA using the Kruskal-Wallis test accompanied by Dunn's Multiple Comparison Test or a two-way ANOVA Prism version 5.0; GraphPad Software. Statistical significance is indicated as follows in the figures: ***P<0.001; **P<0.005; *P< 0.05; and ns, nonsignificant (P>0.05). A spearman correlation matrix was generated based on clinical parameters and gene expression.

4. Results

The aim of the project was to examine whether expression of the ICAM-1 gene in breast cancer cell lines could be induced by cytokines as might be seen in the inflammatory micro-environment that occurs in breast cancer. Western blotting was performed on the stimulated cell lines to confirm the presence of the protein product.

Immunofluorescence was performed to examine the protein in individual cells. Turning to human specimens, qPCR was performed on a series of breast cancer specimens that had histological tissue from the cancer. ICAM-1 expression was evaluated in the human breast cancer specimens and immunohistochemistry for the ICAM-1 protein was performed on FFPE from these samples was performed to look for protein expression. In addition, the FFPE tissue was examined for macrophages with CD68 immunohistochemistry.

4.1 Breast cancer cell lines qPCR and Western Blot analysis

The cells were stimulated in six well plates for 0, 3, 6, 12, 24 and 48 hours. The cytokine concentrations were 50ng/ml for IFN γ , 5ng/ml for TNF α , 25ng/ml for IL1 β and 16ng/ml for IFN α .

4.1.1. MCF7

IFN γ stimulation

The gene expression of ICAM-1 in MCF-7 breast cancer cells stimulated with IFN γ was significantly increased when compared with the control samples. The expression increased by the six-hour time point, when the relative fold change was 10 and stayed elevated at the last time point measured (72 hours). The difference was significant at 3

hours, with a p value of <0.5 and highly significant for 6, 12, 24 and 48-hour time points, with p values <0.01. (Figure 4.1A).

When compared with the 0-hour control sample, the 3 and 6-hour control samples showed fold changes of approximately 3 and 4, respectively, before dropping below 2 for the remainder of the time points. The differences did not have statistical significance, except at 6 hours when the p value was <0.01. (Figure A1)

Western blotting performed on protein harvested from the cell samples stimulated with IFN γ showed weakly staining band at 6, 12, 24, 48 and 72 hours. (Figure 4.1E).

TNF α stimulation

The gene expression of ICAM-1 in MCF-7 breast cancer cells stimulated with TNF α was significantly increased compared to control samples. There was a large increase noted at 3 hours (50-fold change) followed by a second, smaller peak (20-fold change) at 48 hours. The observed difference showed P values of <0.5 at 6 hours and <0.01 for 3, 12, 24 and 48 hours. (Figure 4.1b)

When compared with the 0-hour control sample, the 6-hour control sample showed a fold change of approximately seven. The remainder of the control time points showed fold changes of less than 2. The p-value for the difference at 6 hours was <0.01 and not significant for all other time points. (Figure A1)

Western blotting performed on protein harvested from cell samples stimulated with TNF α showed staining of bands in the 24 and 48 hour samples. Earlier time points were not tested. (Figure 4.1F)

IL1 β stimulation

The MCF-7 cells stimulated with IL1 β showed a large response with approximately 110 fold change after 3 hours which then reduced to about 16 fold change at 6 hours and a fold change of 10 until 48 hours. All of these differences showed significance with P values < 0.001. (Figure 4.1 C)

An additional experiment was run to investigate time-points less than three hours. This showed a large increase at the 2 and 3-hour mark (40-fold change). (Figure A1)

When compared with the 0-hour control sample, the control samples at all the other time points showed fold changes of less than 2. There were no significant differences between these groups. (Figure A1)

Western blotting performed on protein harvested from the cell samples stimulated with IL-1 β showed staining of bands consistent with ICAM-1 at the 12, 24 and 48-hour time points. Earlier samples were not tested. (Figure 4.1G)

IFN α stimulation

The MCF-7 cells stimulated with IFN α showed no significant change in expression over the 48-hour period examined. (Figure 4.1D) When compared with the 0-hour control sample, the 3-hour control sample showed a fold change of 2.16 and the 6-hour control sample showed a fold change of 2.06. All other time points showed fold changes of less than 2. (Figure A1)

Western blotting performed on protein harvested from the cell samples stimulated with IFN α did not show any positive staining. (Figure 4.1F)

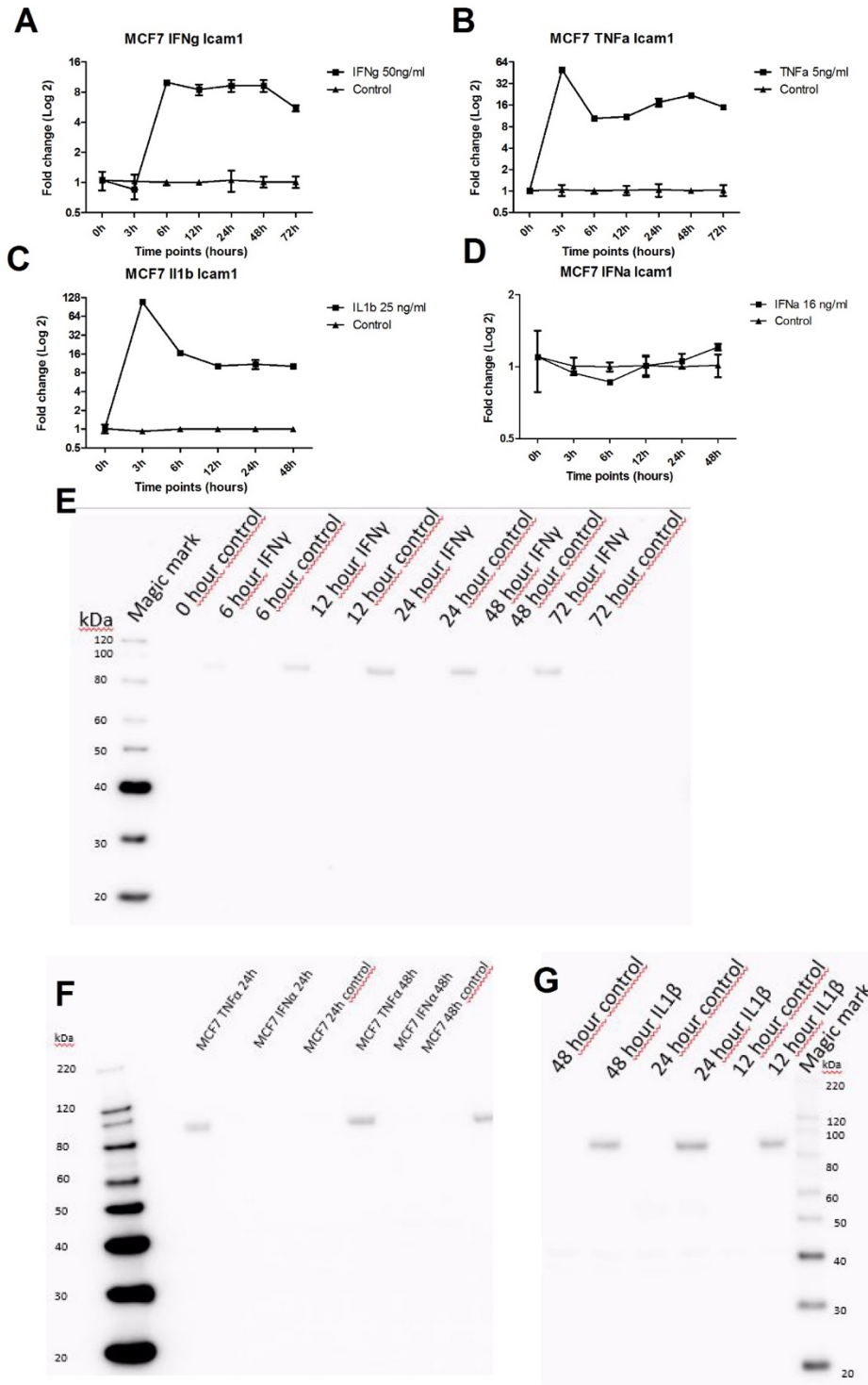


Figure 4.1, A-D: Gene expression of ICAM-1 in MCF7 cell lines stimulated with IFN γ (A), TNF α (B), IL-1 β (C) and IFN α (D). qPCR detecting ICAM-1 was performed on RNA isolated from cell lines stimulated with named cytokines. Expression levels of ICAM-1 were normalised against the expression level of TBP and RPLPO. Data is given as Log 2 of mean SEM of fold change values normalised against time-matched unstimulated control groups. E,F,G: Western blot detection of ICAM-1 on protein extracts from MCF7 cells stimulated with IFN γ (E), TNF α and IFN α (F) and IL1 β (G).

4.1.2. SK-BR-3 cell line

IFN γ stimulation

The SK-BR-3 cells stimulated with IFN γ showed an increased expression of ICAM-1 with a 42.67 fold change at 3 hours increasing to 136.47 fold change at 12 hours and 103.57 fold change at 48 hours. The differences were statistically significant with p-values for the differing time points all being <0.001. (Figure 4.2A)

When compared with the 0-hour control sample, the 3- hour control sample showed a fold change of 3.2 and all other time points showed fold changes of less than 2. None of the differences was statistically significant. (Figure A2)

Western blotting performed on protein harvested from SKBR3 cell samples stimulated with IFN γ showed staining of bands in the 12-hour samples. Other time points were not tested. (Figure 4.2E)

TNF α stimulation

The SK-BR-3 cells stimulated with TNF α showed an increased expression of ICAM-1 with a 34.3-fold change at 3 hours increasing to a 69-fold change peak at 6 hours and decreasing to 18-fold change at 48 hours. Each time point showed a significant difference with p values <0.001. (Figure 4.2B)

When compared with the 0-hour control sample, the control samples at other time points all showed fold changes of less than 2. (Figure A2)

Western blotting performed on protein harvested from SKBR3 cell samples stimulated with TNF α showed staining of bands in the 12-hour samples. Other time points were not tested. (Figure 4.2E)

IL1 β stimulation

The SK-BR-3 cells stimulated with IL1 β showed a peak expression of 135-fold change at 3 hours, which decreased over the time-points, harvested in this experiment and remained elevated at 23 after 48 hours. (Figure 4.2C)

When compared with the 0-hour control sample, the 3-hour control sample showed a fold change of 2, the 6-hour time point showed a fold change of 2.2 and all other time points showed fold changes of less than 2. (Figure A2)

Western blotting performed on protein harvested from SKBR3 cell samples stimulated with IL-1 β showed staining of bands in the 12, 24 and 48-hour samples. (Figure 4.2F)

IFN α stimulation

The SK-BR-3 cells stimulated with IFN α showed elevated ICAM-1 gene expression with fold changes between 5 and 11. All of the sampled time-points showed elevated levels of expression and significant changes with p values of <0.001. (Figure 4.2D)

Compared to the 0-hour control, the 3-hour control showed a fold change of 2.9, the 6-hour control showed a fold change of 2.2 and the fold change for the remaining control time points was less than 1. (Figure A2)

Western blotting performed on protein harvested from SKBR3 cell samples stimulated with IFN α showed no staining in the 12, 24 and 48-hour samples. (Figure 4.2G)

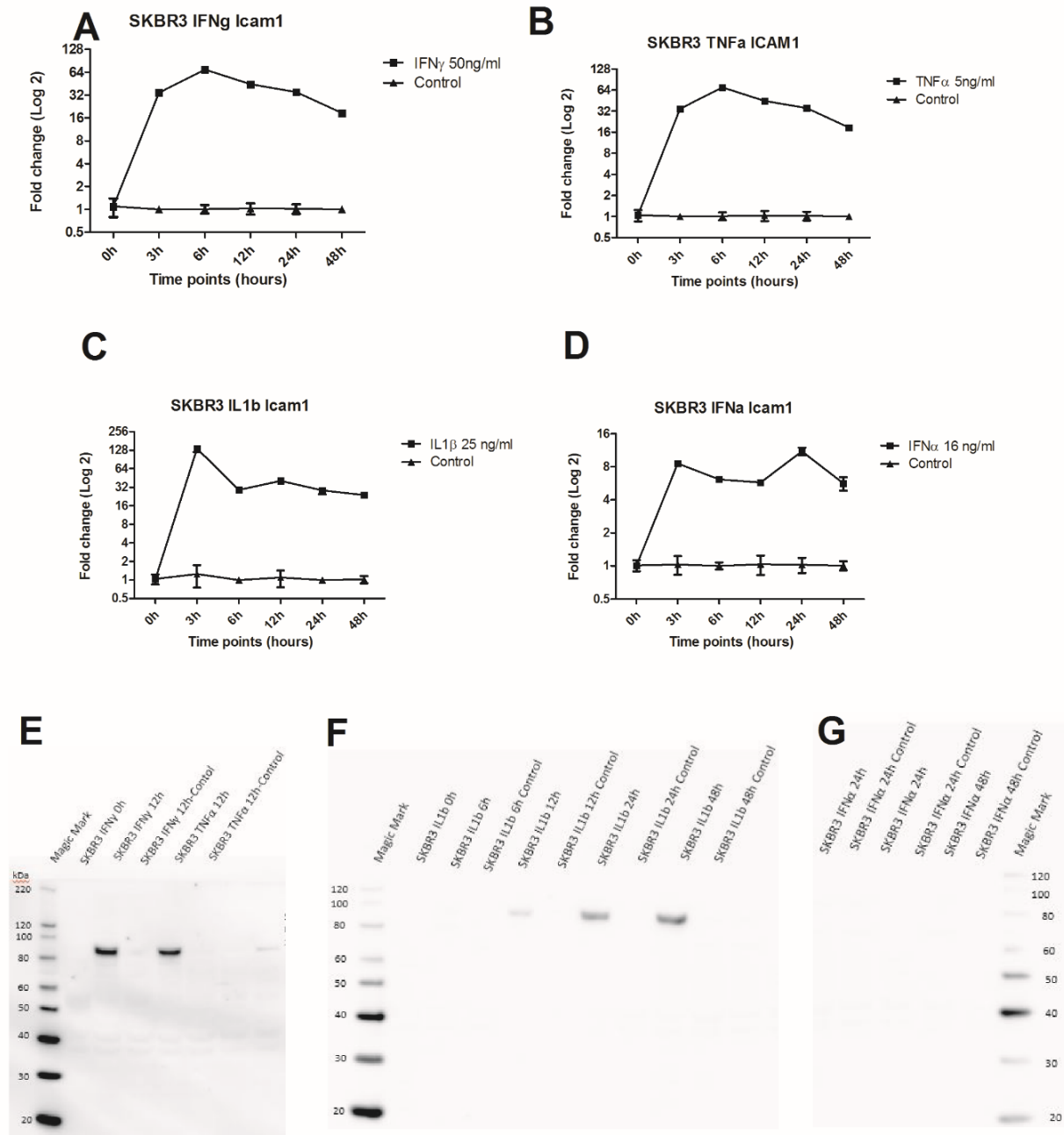


Figure 4.2, A-D: Gene expression of ICAM-1 in SK-BR-3 cell lines stimulated with IFN γ (A), TNF α (B), IL-1 β (C) and IFN α (D). qPCR detecting ICAM-1 was performed on RNA isolated from cell lines stimulated with named cytokines. Expression levels of ICAM-1 were normalised against the expression level of TBP and RPLPO. Data is given as Log 2 of mean SEM of fold change values normalised against time-matched unstimulated control groups. E,F,G: Western blot detection of ICAM-1 on protein extracts from SK-BR-3 cells stimulated with IFN γ and TNF α (E), IL1 β (F) and IFN α (G).

4.1.3. MDA-MB-468 cell line

IFN γ stimulation

The MDA-MB-468 cell line stimulated with IFN γ showed increased ICAM-1 expression of 31-fold change at 3 hours increasing to a peak of 61-fold change at 6 hours and decreasing to 5-fold change at 48 hours. The difference only showed significance by 2-way ANOVA test at 6 hours with a p value of less than 0.01. (Figure 4.3A)

Relative to the fold change at 0 hours, the fold change of the control samples increased over time without stimulation with the largest fold change being 33 at 24 hours. None of these differences was significant. (Figure A3)

Western blotting performed on protein harvested from MDA-MB-468 cell samples stimulated with IFN α showed strong staining in the 12 and 24-hour stimulated samples with weak staining present in the control samples from these time points. (Figure 4.3E)

TNF α stimulation

The MDA-MB-468 cells line stimulated with TNF α showed increased expression of the ICAM-1 gene with a fold change of seven at 3 hours that peaked at 14 at 12 hours and reduced to four at 48 hours. The differences at 3, 6, 12 and 24 hours showed p values of <0.001 and a p value of <0.05 for 48 hours. (Figure 4.3B)

Compared to the 0-hour control, the 3-hour control showed a fold change of 2.2. All the other fold change values were less than two. None of these differences was significant. (Figure A3)

Western blotting performed on protein harvested from MDA-MB-468 cell samples stimulated with TNF α showed strong staining was present in the 12 and 24-hour stimulated samples with weak staining present in the control samples from these time points. (Figure 4.3E)

IL1 β stimulation

The MDA-MB-468 cells stimulated with IL1 β showed an increased expression with the highest value being a 17-fold change at 3 hours, followed by a 10-fold change at 6 hours, dipping to 5-fold change at 12, 24 hours, and an 8-fold change at 48 hours. The differences at 3, 6 and 48 hours showed significance of p value <0.001. At 12 and 24 hours the p value was <0.05. (Figure 4.3C)

All of the control samples showed fold changes less than 2, relative to the 0h control value. (Figure A3)

Western blotting performed on protein harvested from MDA-MB-468 cell samples stimulated with IL1 β showed strong staining was present in the 12 and 24-hour stimulated samples with weak staining present in the control samples from these time points. (Figure 4.3E)

IFN α stimulation

The MDA-MB-468 cells stimulated with TNF α showed no increase in ICAM-1 expression at 3, 6 and 12 hours. There was increased expression of 2.3 fold at 24 hours and 2.6 fold at 48 hours. None of these differences were statistically significant by 2-way ANOVA testing (p>0.5). (Figure 4.3D)

Compared to the 0h control, the control samples showed a 6-fold change expression at 3 hours and a 4-fold change expression at 6 hours. The fold change was less than 2 for the 12, 24 and 48-hour time points. (Figure A3)

Western blotting performed on protein harvested from MDA-MB-468 cell samples stimulated with IFN α showed faint staining in the 12, 24 and 48-hour samples and weaker staining in the corresponding controls. (Figure 4.3E)

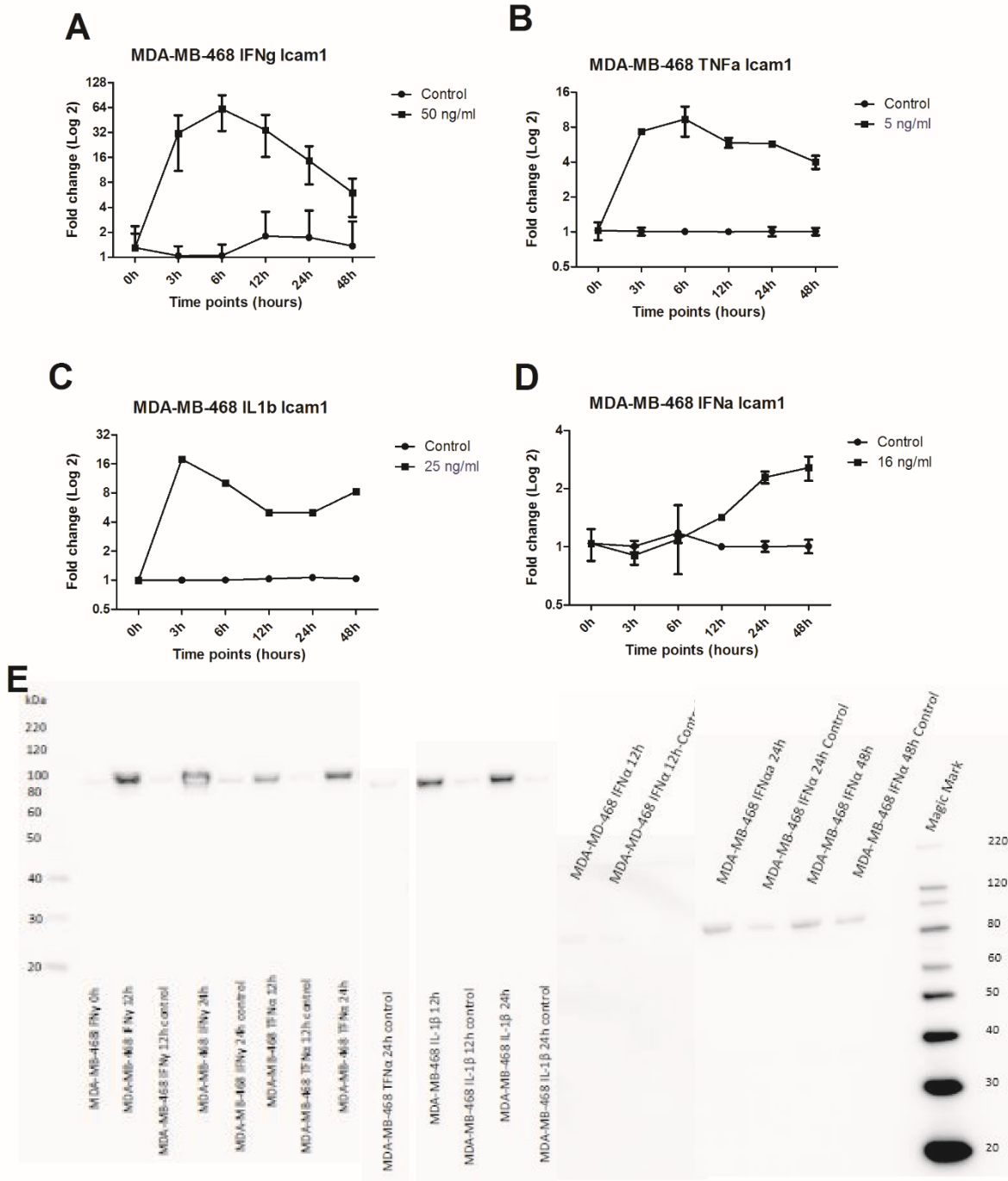


Figure 4.3, A-D: Gene expression of ICAM-1 in MDA-MB-468 cell lines stimulated with IFN γ (A), TNF α (B), IL-1 β (C) and IFN α (D). qPCR detecting ICAM-1 was performed on RNA isolated from cell lines stimulated with named cytokines. Expression levels of ICAM-1 were normalised against the expression level of TBP and RPLPO. Data is given as Log 2 of mean SEM of fold change values normalised against time-matched unstimulated control groups. E: Western blot detection of ICAM-1 on protein extracts from SK-BR-3 cells stimulated with IFN γ , TNF α , IL1 β and IFN α .

Comparing 0-hour expression between the three cell lines

When compared between the three cell lines, no significant differences in ICAM-1 gene expression were identified at 0 hours (data not shown).

4.2. Immunofluorescence on cell lines

Immunofluorescence for ICAM-1 was performed on cells cultured in 8-well slides with removable gaskets. The cells were stimulated for IFN γ , TNF α and IL1 β . A positive control was staining for vimentin. CellTracker Green™ CMFDA (Invitrogen) was used to identify the cytoplasm and DAPI (Invitrogen) to highlight the nucleus.

Positive staining for ICAM-1 was identified in MDA-MB-468 cells (Figures 4.5 to 4.7) and MCF7 cells (Figure 4.4). No staining was seen in the SK-BR-3 stimulated cells. The staining was seen in the well stimulated with IFN and the well that was not stimulated. No staining was seen in the wells stimulated with TNF α or IL1 β . Not all of the cells in a well stained. At most 20% staining was seen in the MDA-MB-468 control well, approximately 10% in the MDA-MB-468 well stimulated with IFN γ and approximately 5% in the MCF7 unstimulated well and well stimulated with IFN γ .

Two staining patterns were observed. The most common pattern was membranous staining with a fine outline to the cell (Figures 4.5, 4.7). A second pattern took the appearance of a para-nuclear globule (Figure 4.6).

Vimentin staining highlighted the cell cytoskeleton. (Figure 4.4)

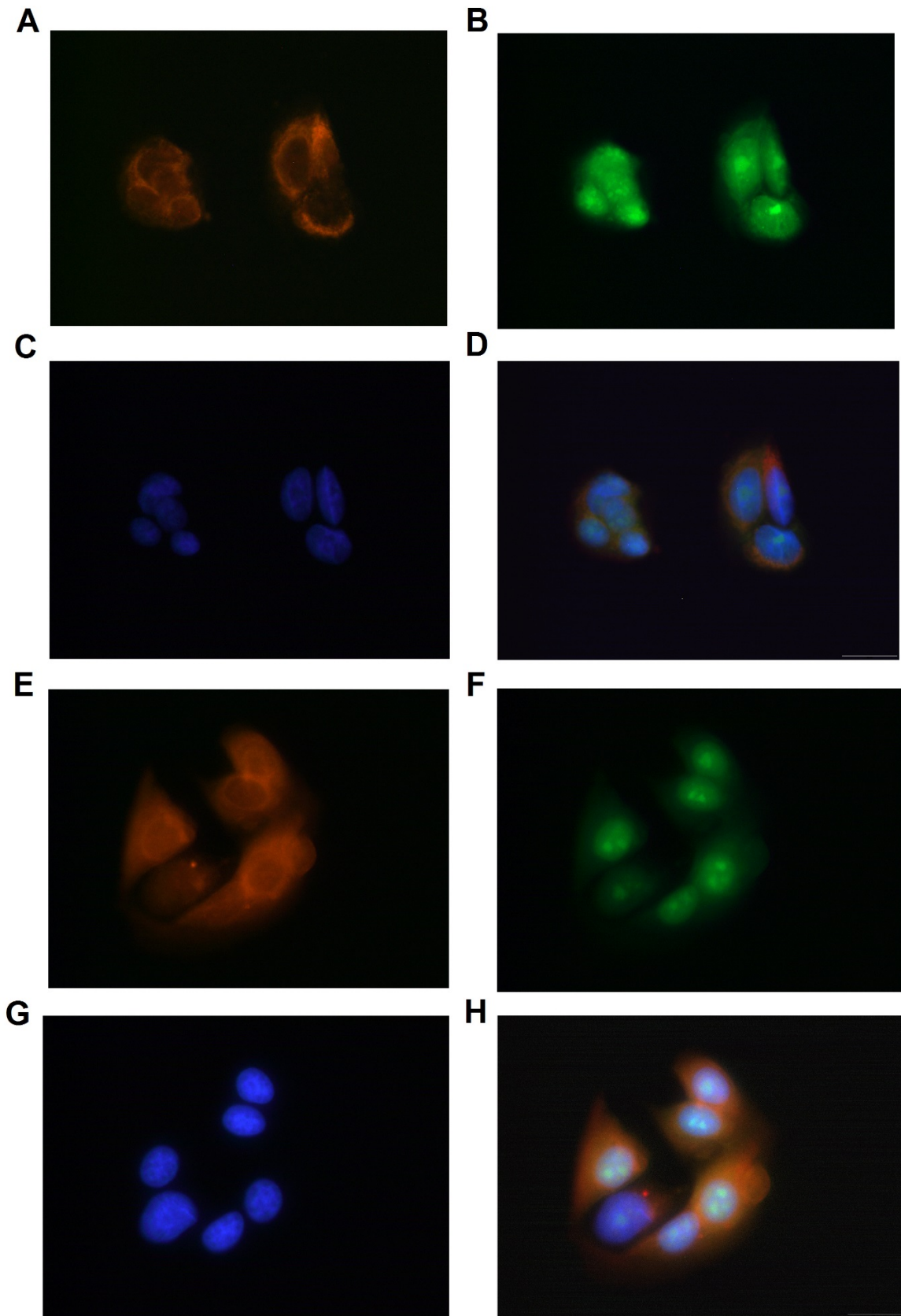


Figure 4.4 Immunofluorescence staining for ICAM-1(A-D) and vimentin (E to H) in MCF7 cells. A and E show Alexa Fluor 546 secondary antibody signal, B and F highlight cytoplasm with Cell Tracker Green™, C and H show nuclear staining with DAPI, D and H are composite images. High magnification (600x).

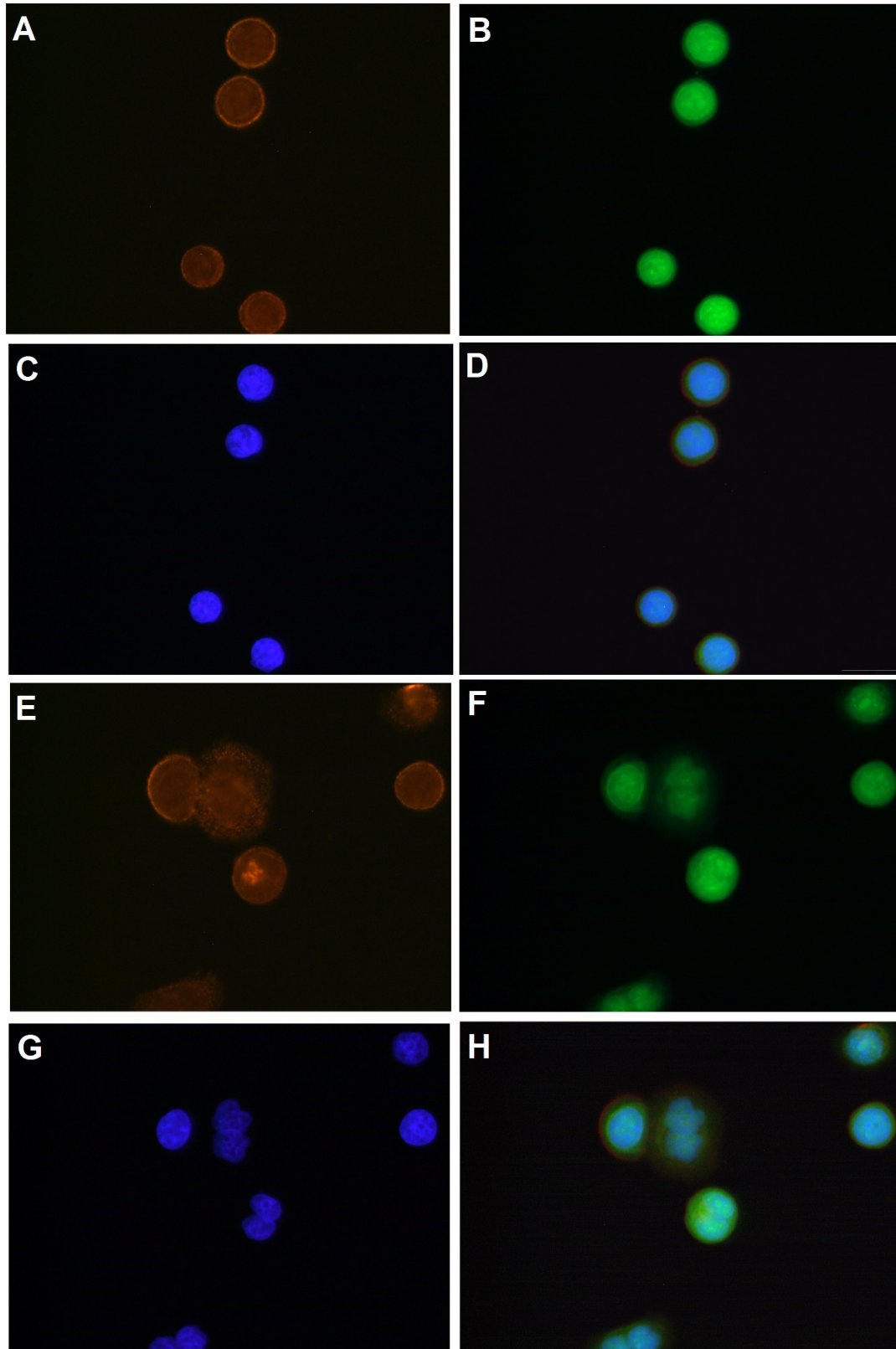


Figure 4.5 Immunofluorescence staining for ICAM-1 in MDA-MB-468 cells. A and E show Alexa Fluor 546 secondary antibody signal, B and F highlight cytoplasm with Cell Tracker Green™, C and H show nuclear staining with DAPI, D and H are composite images. Both series were stimulated with IFN γ . High magnification (A-D 400x, E-H 600x)

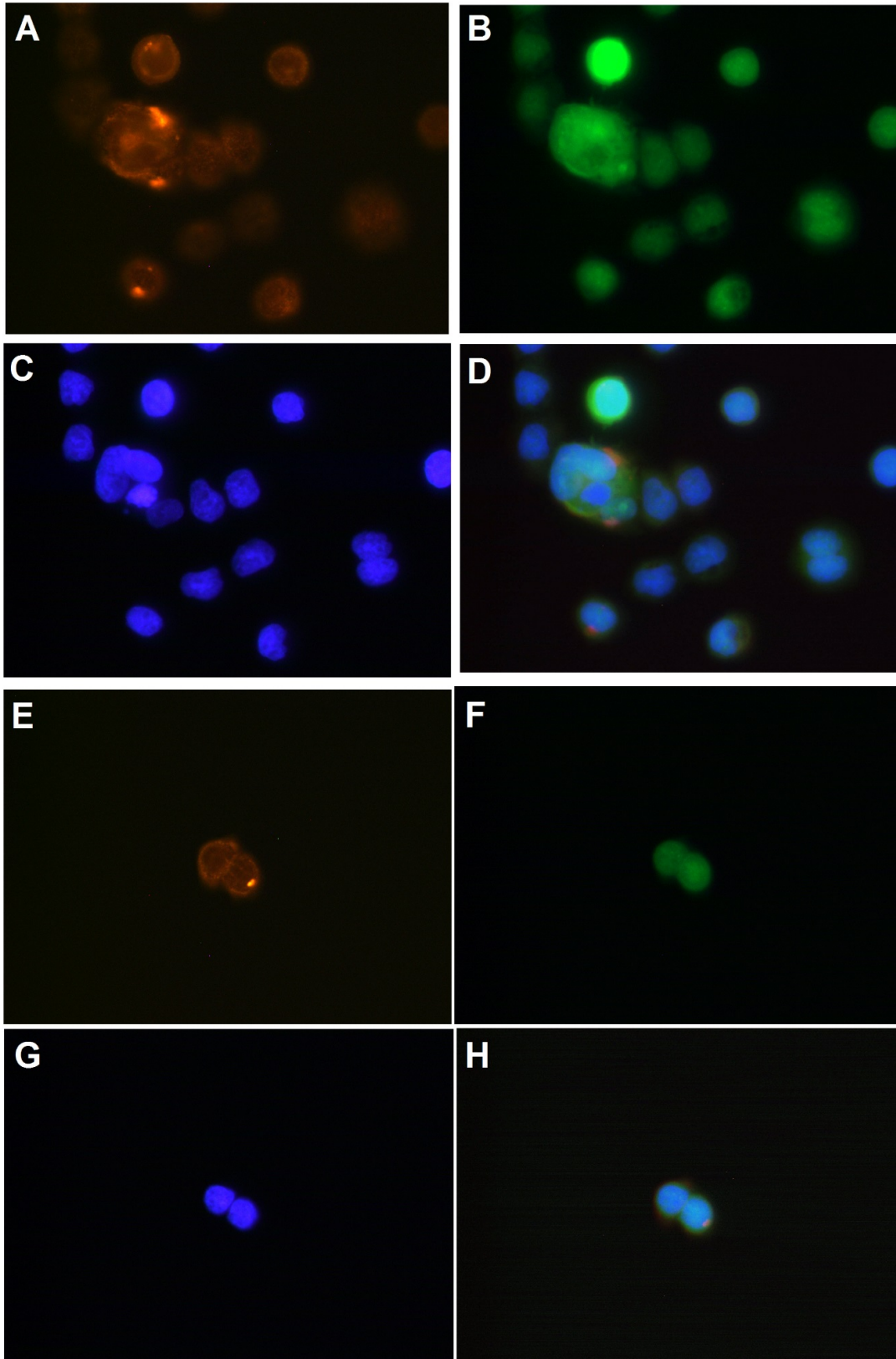


Figure 4.6 Immunofluorescence staining for ICAM-1 in MDA-MB-468 cells. A and E show Alexa Fluor 546 secondary antibody signal, B and F highlight cytoplasm with Cell Tracker Green™, C and H show nuclear staining with DAPI, D and H are composite images. Both series were stimulated with IFN γ . High magnification (400x).

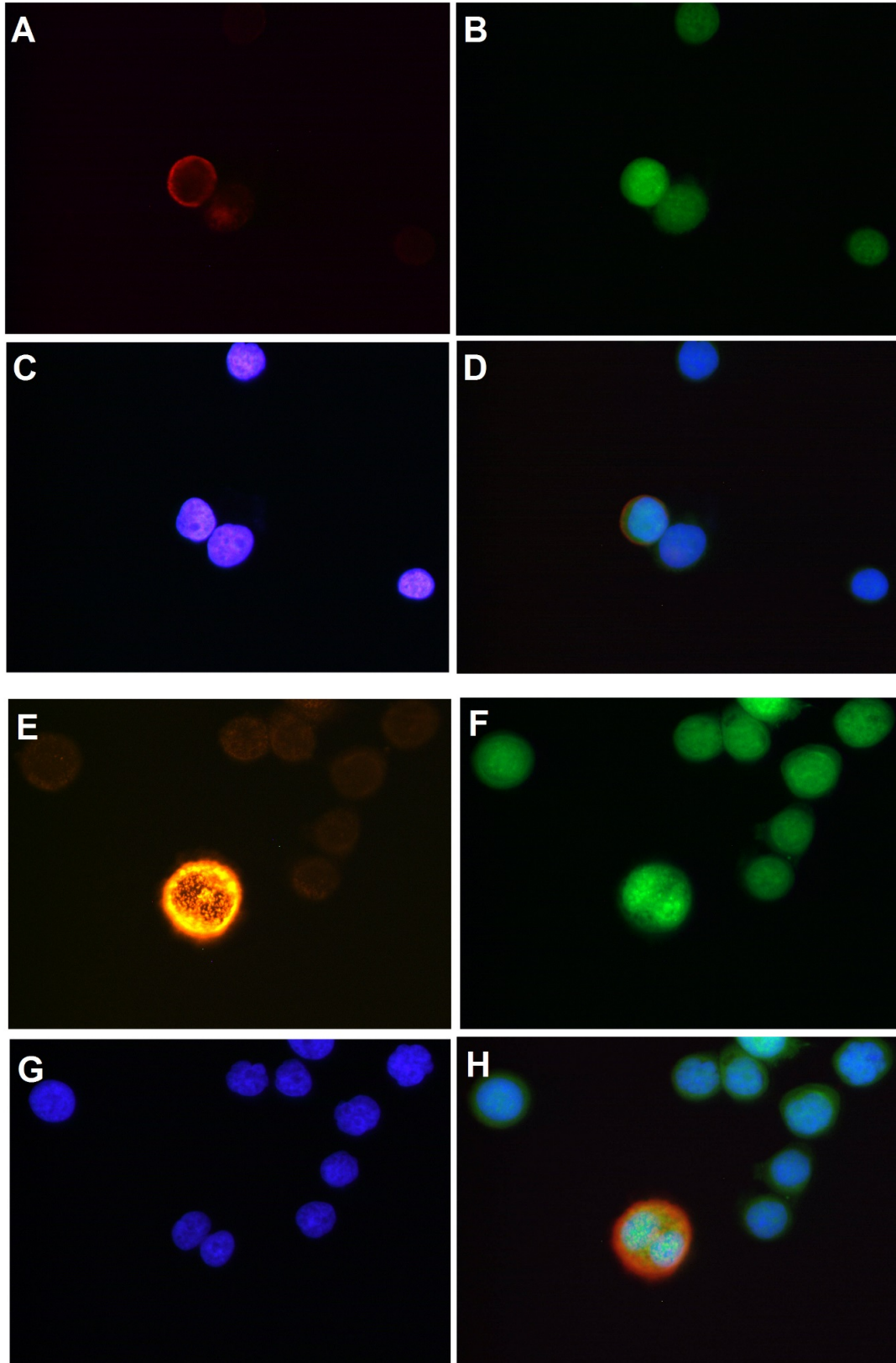


Figure 4.7 Immunofluorescence staining for ICAM-1 in MDA-MB-468 cells. A and E show Alexa Fluor 546 secondary antibody signal, B and F highlight cytoplasm with Cell Tracker Green™, C and H show nuclear staining with DAPI, D and H are composite images. Both series were from an unstimulated well. High magnification (600x)

4.3. Human tumour specimens

4.3.1. qPCR

The quantitative real time PCR results from the human tumour samples showed increased ICAM-1 expression in tumour samples compared to matched normal samples (N). The significant difference was present when the gene expression was normalised to the average of the matched normal tissue (avg N) and to unmatched normal breast tissue taken from different patients (avg NN). The matched normal tissue RNA was isolated from macroscopically normal appearing tissue in the vicinity of breast cancer in a surgical specimen. The unmatched normal tissue was taken from breast specimens that were not operated on for neoplastic disease.

There increased expression in the tumour samples when compared to normal samples showed a range from 0.58-fold change to 27.10-fold change.

A two tailed student T-test comparing the ICAM-1 levels from the tumour samples normalised against the matched normal tissue (avg N) showed a significant difference with a p-value of 0.0017 (Figure 4.7 Icam1 norm avg N). A two tailed student T-test comparing the ICAM-1 levels from the tumour samples normalised against unmatched normal tissue (avgNN) gave a p-value of less than 0.0001 (Figure 4.7, ICAM1 norm avg NN).

The expression of other genes of interest were tested on the same samples to validate the ICAM1 expression (Figure A4). Only the CCR7 and LT β gene expression were significantly increased in the tumour samples compared to the normal samples ($p < 0.001$ and $p < 0.01$, respectively, Figure A4). Interestingly, the expression of IFN α was significantly decreased in the tumour samples ($p < 0.01$, Figure A4).

A spearman correlation matrix was generated comparing the gene expression data and the clinical parameters listed in Table A1 (Table A2 and A3). The results demonstrated a positive correlation in the tumour samples between the ICAM1 expression and the

expression of the chemokine CCL19 and the chemokine receptors CCR5 and CXCR5 (Table A2 and A3). No correlation between the ICAM1 expression and the ER, PGR and HER2 status of the tumour samples were found (Table A2 and A3).

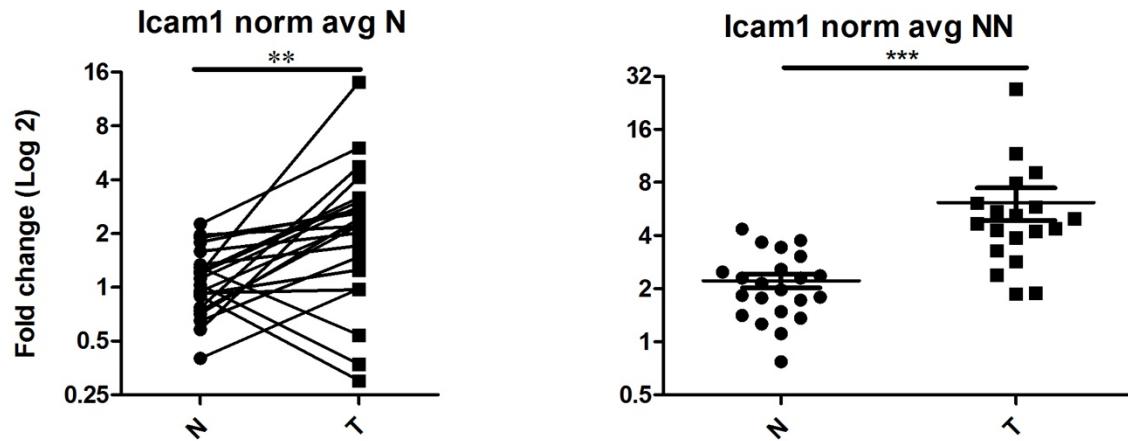


Figure 4.7. Gene expression of ICAM-1 normalised against the average of matched normal tissue from the same patient (N) or the average of normal tissue from patients without breast cancer (NN). Significant differences marked *** $P < 0.001$, ** $P < 0.01$.

4.3.2. Immunohistochemistry

4.3.2.1. Macrophages (CD68)

The 23 breast cancer cases previously used for deep sequencing were stained for CD68. A semi-quantitative assessment of the number of macrophages was made by a single observer who was blinded to the clinical details of the case. The number of macrophages were assessed as none (0), scant (+), moderate (++) and frequent (+++). All of the tumours showed some staining with CD68. CD68 staining was generally seen most frequently at the edge of the tumour, often as a band-like zone at the tumour/stromal interface (Figure 4.8). CD68 positive cells with morphology consistent with macrophages were present within the tumour, often scattered amongst the intra-tumoural stroma. It was rare to find CD68 positive cells within tumour nests in direct contact with tumour cells.

6/23 (26%) of tumours were in the scant (+) group, 10/23 (44%) were in the ++ group and 7/23 (31%) were in the +++ group. (Table 4.1)

A single case was stained for CD168, another macrophage marker. This antibody appeared to react with two populations of cells; both those with the appearance of macrophages and elongated cells in fibrous tissue whose appearance was consistent with fibroblasts (data not shown).

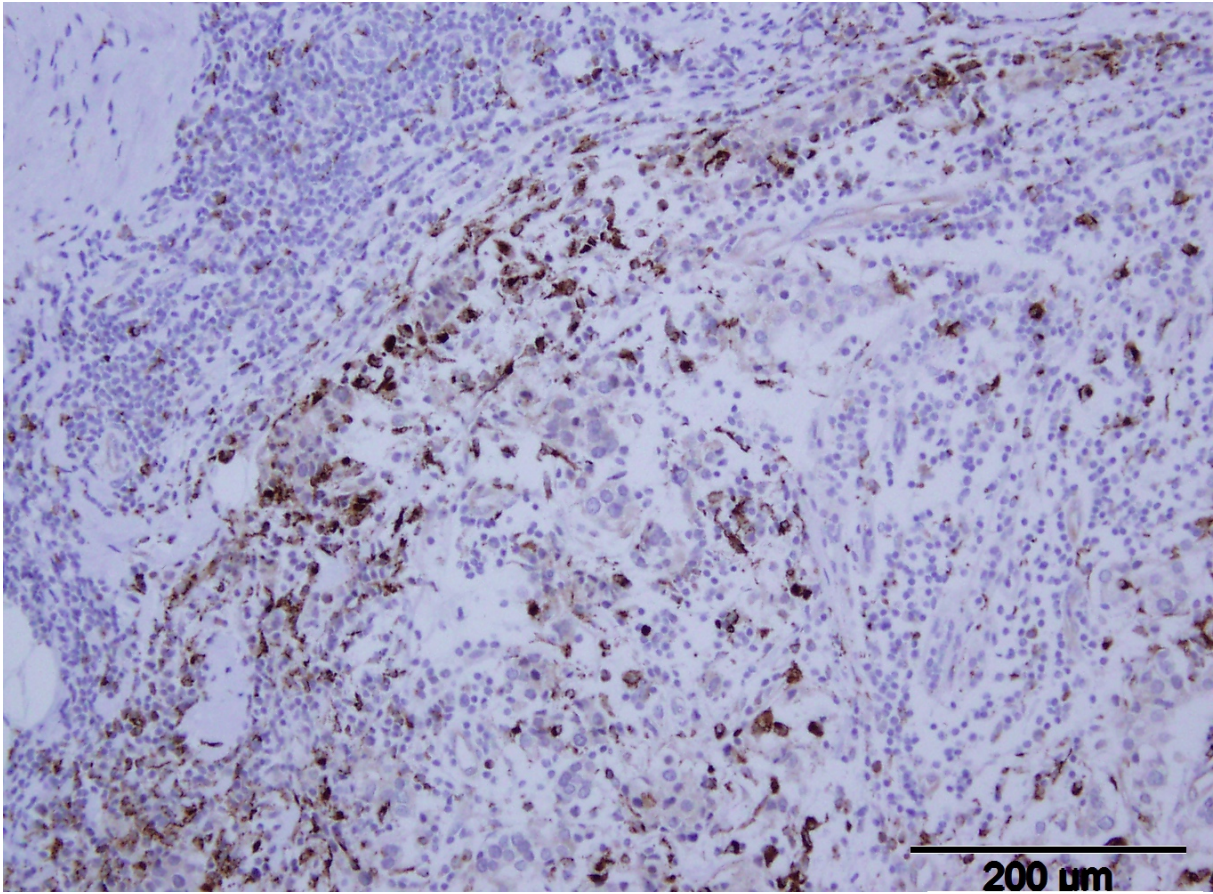


Figure 4.8. CD68 immunohistochemistry showing macrophages both at the advancing edge of the tumour and scattered within it. Low power (100x).

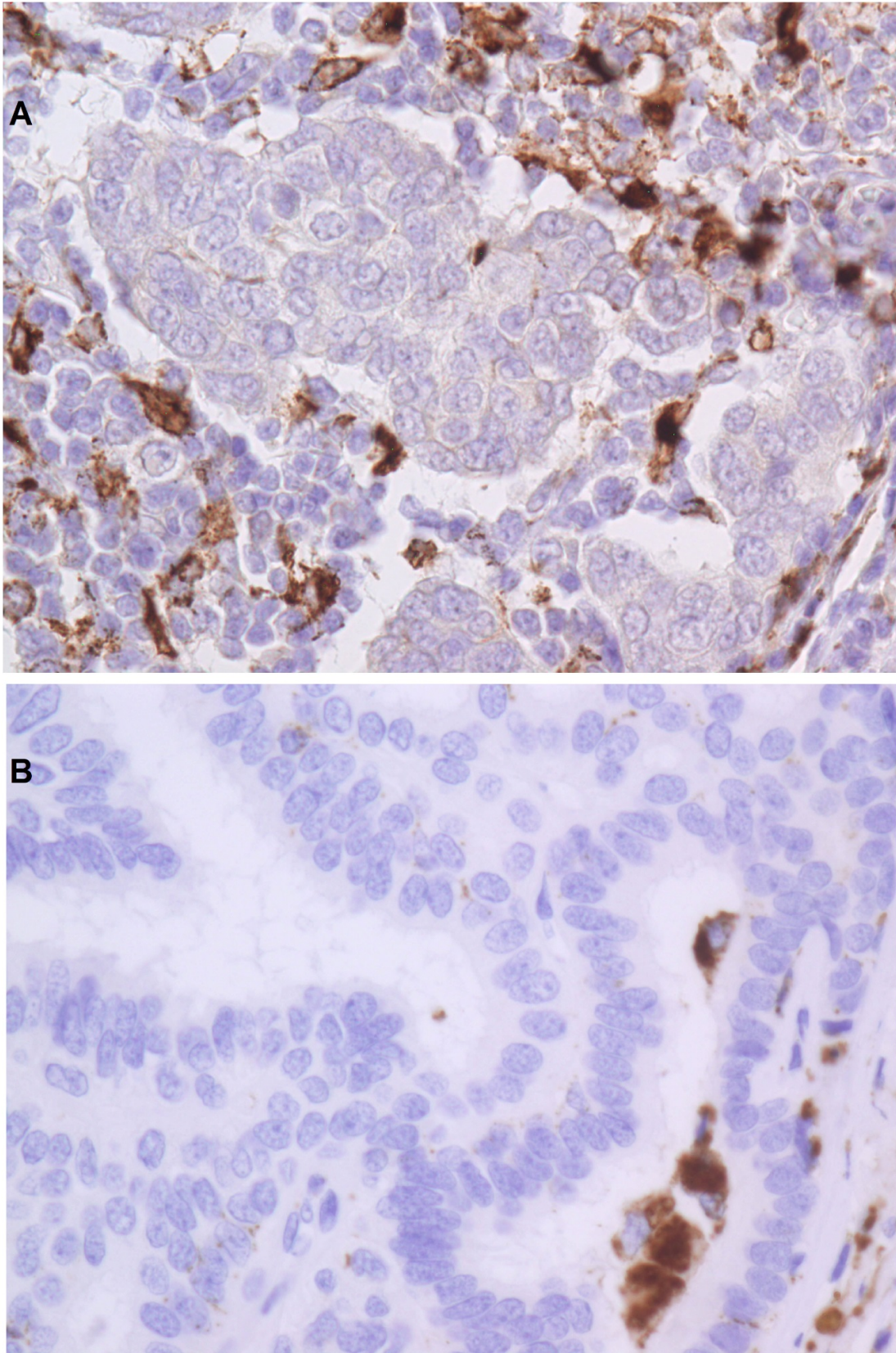


Figure 4.9. Higher power view (400x) of CD68 positive cells within the tumour mass where they mainly were found outside of tumour nests, commonly in tumour stroma (A). Some macrophages were present in glandular lumen (B).

Table 4.1. Comparison of staining of FFPE tissue from deep sequenced breast cancer patients with macrophage frequency (CD68), ICAM-1 positivity in the tumour and ICAM-1 qPCR results.

Tumour number	Macrophage Immunohistochemistry	ICAM-1 Immunohistochemistry	ICAM-1 fold change normalised to NN
1	+	No staining	27.10
3	++	<5% staining of tumour	6.11
4	++	<1% staining of tumour	3.29
6	+	No staining	1.89
7	+++	No staining	4.99
9	++	No staining	5.46
10	++	No staining	4.29
11	++	<25% of tumour staining	0.58
12	+	<5% of tumour staining	2.30
13	+++	<1% of tumour staining	9.13
15	+++	No staining	11.63
16	++	No staining	1.05
17	++	No staining	3.89
18	++	No staining	2.85
20	+++	No staining	0.70
21	++	No staining	4.38
22	+++	No staining	5.21
24	++	No staining	2.39
25	+	No staining	4.66
26	+	No staining	5.82
27	+++	<5% of tumour staining	4.23
30	++	No staining	7.94
31	+++	No staining	1.87

4.3.2.2. ICAM-1 immunohistochemistry

None of the 23 tumour samples showed strong uniform staining with ICAM-1 as would be expected with positive immunohistochemistry. 7 of the 23 tumour samples showed some evidence of ICAM-1 staining in the tumours (Table 4.1). Most of this staining was moderate or less in intensity and of 5% or less of the cells. Some tumours had relatively strong membranous staining in areas which appeared to be in-situ neoplastic disease.

All of the sections examined showed some ICAM-1 staining in some normal tissue structures including the endothelium of small and medium sized blood vessels and staining of a subset of immune cells (data not shown). Some samples showed areas of fat necrosis and the macrophages in these areas appeared to show weak membranous ICAM-1 staining (data not shown).

No relationship could be identified between the ICAM-1 qPCR gene expression results, ICAM-1 immunohistochemistry or CD68 immunohistochemistry.

An extra set of eight breast cancer cases were stained for ICAM-1. One of these showed strong positive staining (Figure 4.10). This case was triple negative in its staining pattern for oestrogen receptor, progesterone receptor and HER-2. (ER -ve, PR-ve, HER2 -ve).

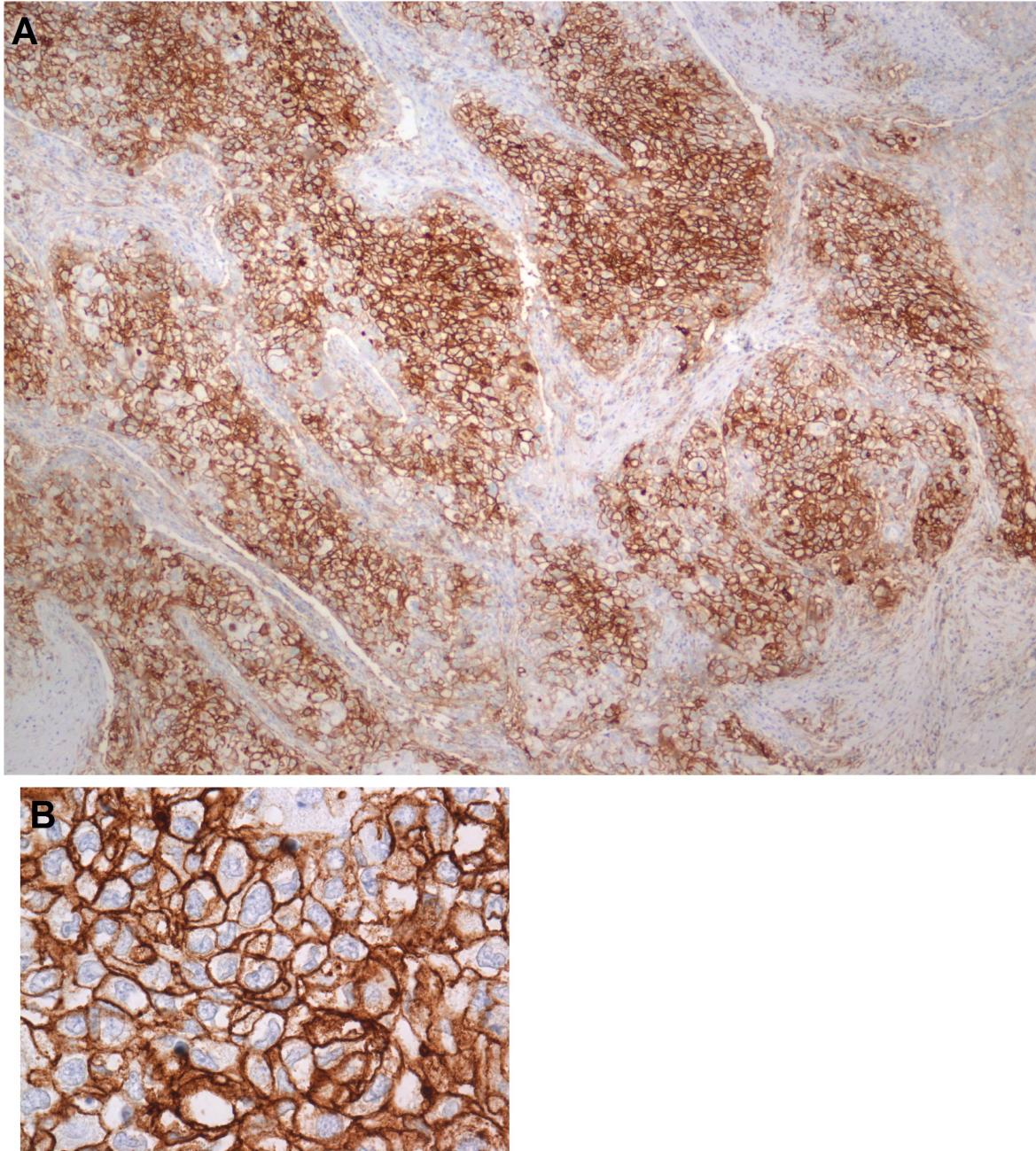


Figure 4.10. Immunohistochemistry for ICAM-1 showing a positive breast cancer case (not part of the cohort that underwent qPCR for ICAM1). The majority of the tumour cells appear positive (A, 40x). Higher power confirms membranous staining (B, 400x).

5. Discussion

The cell culture experiments showed that stimulation by certain cytokines can cause a significant increase in expression of the ICAM-1 gene in breast cancer cells and that this increased expression leads to the production of ICAM-1 protein. There was some similarity in the pattern of expression elicited by the cytokines. $\text{IFN}\gamma$, $\text{TNF}\alpha$ and $\text{IL-1}\beta$ caused an increase in expression in most cell lines. $\text{IFN}\alpha$ only caused an increase in expression in the SK-BR-3 cell line and this increased expression was less than that seen in the other stimulations for that cell line. These findings are consistent with those of Hutchins and Steel [54] who found that $\text{IFN}\gamma$, $\text{TNF}\alpha$, $\text{IL-1}\beta$ and also $\text{IL-1}\alpha$ and IL6 upregulated the expression of ICAM-1 in four breast cancer cell lines (T47D, ZR-75-1, MCF7D and HS578T). That experiment used flow cytometry to examine the expression of cell surface markers in breast cancer cell lines. Another study examining ICAM-1 in breast cancer cell lines reported that ICAM-1 expression was reduced in ZR-75-1, MCF7D and SK-BR3 compared to a benign mammary cell line (HBL-100) and that $\text{TNF}\alpha$ but not $\text{IFN}\gamma$ was able to raise level of expression [55]. $\text{IFN}\alpha$ was tested in this paper and did not raise gene expression suggesting that the increase seen in this project may have been an error, especially as protein levels were not increased.

In general, $\text{IL-1}\beta$ caused an early induction of ICAM-1 with a very high peak at 3 hours of approximately 128-fold change in the MCF7 cell line and the SK-BR-3 cell line. The response in the MDA-MB-468 cell line was less with a 16-fold change at 3 hours. Repeating the stimulation with earlier time points with MCF7 cells suggested that the raised level of expression might peak even earlier, at two hours.

$\text{TNF}\alpha$ caused a larger induction of ICAM-1 expression in the SK-BR-3 cell line and in the MCF7 cell line than in the MDA-MB-468 cell line.

$\text{IFN}\gamma$ caused a larger induction of ICAM-1 expression in the SK-BR-3 cell line and the MDA-MB-468 cell line than in the MCF-7 cell line.

Constitutive ICAM-1 expression is regulated by a balance of enhancing and silencing factors [56]. Increased expression by IFN and IL-6 is through binding of transcription factors to a palindromic response unit [57] and glucocorticoid repression also occurs at the transcriptional level [58].

The differing responses to the same stimuli may reflect differing biological function of the cell lines. Other studies have noted decreased ICAM-1 expression in SK-BR-3 and MCF-7 [55] cells or constitutively raised levels as in MDA-MB-468 [59] when compared to non-neoplastic mammary cell expression. Although these expression differences were not proven in this project, they may have been seen if a 'normal' mammary cell line was used as a control or through the use of flow cytometry to examine the surface markers.

In general, the increased ICAM-1 gene expression was matched with production of ICAM-1 protein as measured by Western Blot. An exception to this was seen with SK-BR-3 cells stimulated with IFN α , where no ICAM-1 was detected despite elevated ICAM-1 gene expression in these samples. The expression levels showed a significant difference but of much lower magnitude than that seen with the other cytokines in this cell line; it may be that a larger change in gene expression is required to produce protein in SK-BR-3 cells. The unstimulated controls also increased their ICAM-1 expression suggesting that a problem with the experimental conditions may have occurred (Figure A2). It is of interest that a similar magnitude of gene expression change was seen with IFN γ induction of MDA-MB-468 cells and ICAM-1 protein was detected in that case.

Concerning MDA-MB-468, weak bands were detected in the control samples including at 0-hours. There was also some increased staining relative to the control samples at 24 and 48 hours for IFN α stimulation even though the fold change relative expression was barely over two. Constitutive expression of ICAM-1 has been described previously and may be involved with these results [46].

The immunofluorescence results showed that ICAM-1 protein was present on the membrane of all cell types at 24 hours in non-stimulated cells and in cells stimulated with IFN γ . This does not correlate well with the qPCR or western blot results which would suggest the presence of ICAM-1 in the TNF α and IL-1 β stimulated cells. It is possibly due to a technical error or shedding of the surface protein. The western blot result pools the protein in all the cells in a sample while the immunofluorescence examines the protein in individual cells. The well volume in the gasket slides was different than that plated for cell culture stimulation experiments and it is possible that there were too many cells per well leading to cell stress and expression of ICAM-1 as a response to contact inhibition. Another possibility is that auto-fluorescence might have been misinterpreted as true staining in some wells. The para-nuclear staining is suggestive of a para-nuclear 'hoff' as seen in a plasma cell and may reflect active protein production.

Analysis of the medium that the cells were cultured in was not performed in this project. This could be analysed in the future to give information about the presence of soluble ICAM-1 or cytokines that may have been released by tumour cells secondary to stimulation.

The human tumour samples showed a general increase in ICAM-1 expression but there was some difficulty in determining a good control tissue. The control was macroscopically normal appearing tissue taken from the tissue removed at operation. Although the tissue may not contain tumour cells, it is likely to be involved in any cytokine signalling which presumably extends towards the draining lymph nodes and across some amount of tissue. It seems likely that cytokines acting on cancerous tissue may also be acting upon neighbouring tissue even if in smaller concentrations. Interestingly, the expression of the cytokine IFN α was higher in the normal samples compared to the tumour samples.

The macrophage assessment was performed by one observer, blinded to clinical details. It was performed in the manner of a pilot project but was not subject to evaluation of intra-observer variability or inter-observer variability and lacks rigor due to this. Comparison with the results of another observer and measurement of the concordance between the opinions would improve confidence in the results.

The nature of the cohort available for ICAM-1 immunohistochemistry made interpretation difficult as there were no definitively positive cases among those that had RNA available for qPCR. The case demonstrated in Figure 4.10 was from a separate cohort of cases that did not have RNA available for gene expression analysis. A larger cohort with more ICAM-1 positive cases may allow more firm conclusions to be made in the future. Furthermore, protein could be harvested from human tumour samples for comparison with cell culture results by western blot or enzyme-linked immunosorbent assay (ELISA). ELISA would add information above that provided by Western Blot as it could quantify the protein present.

Conclusion

Breast cancer cell lines stimulated by IFN γ , TNF α and Il-1 β show increased expression of the ICAM-1 gene and its protein product. IFN α shows an increase in ICAM-1 gene expression in SK-BR-3 cells but no increase in protein product. ICAM-1 protein localises to the cell surface and a para-nuclear location in cultured breast cancer cells as seen by immunofluorescence. There is increased expression of ICAM-1 in breast cancer tissue as compared to normal tissue however this is not reflected by protein expression as measured by immunohistochemistry or numbers of macrophages. Considering the hypothesis of ICAM-1-mediated carcinogenesis suggested by Roland [47], this project confirms that cytokines induce ICAM-1 gene expression and protein production but not that macrophages will be attracted to the site to further the neoplastic process.

6. References

1. Cancer Registry of Norway, *Cancer in Norway 2014 - Cancer incidence, mortality, survival and prevalence in Norway*. 2015, Oslo: Cancer Registry of Norway.
2. Yersal, O. and S. Barutca, *Biological subtypes of breast cancer: Prognostic and therapeutic implications*. *World J Clin Oncol*, 2014. **5**(3): p. 412-24.
3. Sreekumar, A., K. Roarty, and J.M. Rosen, *The mammary stem cell hierarchy: a looking glass into heterogeneous breast cancer landscapes*. *Endocr Relat Cancer*, 2015. **22**(6): p. T161-76.
4. Sorlie, T., et al., *Gene expression patterns of breast carcinomas distinguish tumor subclasses with clinical implications*. *Proc Natl Acad Sci U S A*, 2001. **98**(19): p. 10869-74.
5. Santos, C., et al., *Intrinsic cancer subtypes--next steps into personalized medicine*. *Cell Oncol (Dordr)*, 2015. **38**(1): p. 3-16.
6. Bernardo, G.M., et al., *FOXA1 represses the molecular phenotype of basal breast cancer cells*. *Oncogene*, 2013. **32**(5): p. 554-63.
7. Abd El-Rehim, D.M., et al., *Expression of luminal and basal cytokeratins in human breast carcinoma*. *J Pathol*, 2004. **203**(2): p. 661-71.
8. Schnitt, S.J., *Will molecular classification replace traditional breast pathology?* *Int J Surg Pathol*, 2010. **18**(3 Suppl): p. 162S-166S.
9. Rakha, E.A., et al., *Are triple-negative tumours and basal-like breast cancer synonymous?* *Breast Cancer Res*, 2007. **9**(6): p. 404; author reply 405.
10. Badve, S., et al., *Basal-like and triple-negative breast cancers: a critical review with an emphasis on the implications for pathologists and oncologists*. *Mod Pathol*, 2011. **24**(2): p. 157-67.
11. Larsen, P.B., I. Kumler, and D.L. Nielsen, *A systematic review of trastuzumab and lapatinib in the treatment of women with*

- brain metastases from HER2-positive breast cancer. Cancer Treat Rev, 2013. 39(7): p. 720-7.*
12. Martin-Castillo, B., et al., *Basal/HER2 breast carcinomas: integrating molecular taxonomy with cancer stem cell dynamics to predict primary resistance to trastuzumab (Herceptin).* Cell Cycle, 2013. **12**(2): p. 225-45.
 13. Prat, A., et al., *Phenotypic and molecular characterization of the claudin-low intrinsic subtype of breast cancer.* Breast Cancer Res, 2010. **12**(5): p. R68.
 14. Harrell, J.C., et al., *Endothelial-like properties of claudin-low breast cancer cells promote tumor vascular permeability and metastasis.* Clin Exp Metastasis, 2014. **31**(1): p. 33-45.
 15. Prat, A. and C.M. Perou, *Deconstructing the molecular portraits of breast cancer.* Mol Oncol, 2011. **5**(1): p. 5-23.
 16. Lacroix, M. and G. Leclercq, *Relevance of breast cancer cell lines as models for breast tumours: an update.* Breast Cancer Res Treat, 2004. **83**(3): p. 249-89.
 17. Holliday, D.L. and V. Speirs, *Choosing the right cell line for breast cancer research.* Breast Cancer Res, 2011. **13**(4): p. 215.
 18. Rangarajan, A., et al., *Species- and cell type-specific requirements for cellular transformation.* Cancer Cell, 2004. **6**(2): p. 171-83.
 19. Kao, J., et al., *Molecular profiling of breast cancer cell lines defines relevant tumor models and provides a resource for cancer gene discovery.* PLoS One, 2009. **4**(7): p. e6146.
 20. Neve, R.M., et al., *A collection of breast cancer cell lines for the study of functionally distinct cancer subtypes.* Cancer Cell, 2006. **10**(6): p. 515-27.
 21. Hollestelle, A., et al., *Distinct gene mutation profiles among luminal-type and basal-type breast cancer cell lines.* Breast Cancer Res Treat, 2010. **121**(1): p. 53-64.
 22. Kuperwasser, C., et al., *Reconstruction of functionally normal and malignant human breast tissues in mice.* Proc Natl Acad Sci U S A, 2004. **101**(14): p. 4966-71.

23. Burdall, S.E., et al., *Breast cancer cell lines: friend or foe?* Breast Cancer Res, 2003. **5**(2): p. 89-95.
24. Coussens, L.M. and Z. Werb, *Inflammation and cancer*. Nature, 2002. **420**(6917): p. 860-7.
25. DeNardo, D.G. and L.M. Coussens, *Inflammation and breast cancer. Balancing immune response: crosstalk between adaptive and innate immune cells during breast cancer progression*. Breast Cancer Res, 2007. **9**(4): p. 212.
26. Garcia-Tunon, I., et al., *Influence of IFN-gamma and its receptors in human breast cancer*. BMC Cancer, 2007. **7**: p. 158.
27. Ruiz-Ruiz, C., et al., *The up-regulation of human caspase-8 by interferon-gamma in breast tumor cells requires the induction and action of the transcription factor interferon regulatory factor-1*. J Biol Chem, 2004. **279**(19): p. 19712-20.
28. Zaidi, M.R. and G. Merlino, *The two faces of interferon-gamma in cancer*. Clin Cancer Res, 2011. **17**(19): p. 6118-24.
29. Yu, M., et al., *Targeting transmembrane TNF-alpha suppresses breast cancer growth*. Cancer Res, 2013. **73**(13): p. 4061-74.
30. Dinarello, C.A., *The biological properties of interleukin-1*. Eur Cytokine Netw, 1994. **5**(6): p. 517-31.
31. Jin, L., et al., *Expression of interleukin-1beta in human breast carcinoma*. Cancer, 1997. **80**(3): p. 421-34.
32. Gutterman, J.U., *Cytokine therapeutics: lessons from interferon alpha*. Proc Natl Acad Sci U S A, 1994. **91**(4): p. 1198-205.
33. Ferrantini, M., I. Capone, and F. Belardelli, *Interferon-alpha and cancer: mechanisms of action and new perspectives of clinical use*. Biochimie, 2007. **89**(6-7): p. 884-93.
34. Escobar, G., et al., *Genetic engineering of hematopoiesis for targeted IFN-alpha delivery inhibits breast cancer progression*. Sci Transl Med, 2014. **6**(217): p. 217ra3.
35. Dustin, M.L., et al., *Induction by IL 1 and interferon-gamma: tissue distribution, biochemistry, and function of a natural adherence molecule (ICAM-1)*. J. Immunol. 1986. **137**: 245-254. J Immunol, 2011. **186**(9): p. 5024-33.

36. van de Stolpe, A. and P.T. van der Saag, *Intercellular adhesion molecule-1*. J Mol Med (Berl), 1996. **74**(1): p. 13-33.
37. Basoglu, M., et al., *Correlation between the serum values of soluble intercellular adhesion molecule-1 and total sialic acid levels in patients with breast cancer*. Eur Surg Res, 2007. **39**(3): p. 136-40.
38. Maruo, Y., et al., *ICAM-1 expression and the soluble ICAM-1 level for evaluating the metastatic potential of gastric cancer*. Int J Cancer, 2002. **100**(4): p. 486-90.
39. Forsea, A.M., et al., *Melanoma prognosis in Europe: far from equal*. Br J Dermatol, 2014. **171**(1): p. 179-82.
40. Johnson, J.P., et al., *De novo expression of intercellular-adhesion molecule 1 in melanoma correlates with increased risk of metastasis*. Proc Natl Acad Sci U S A, 1989. **86**(2): p. 641-4.
41. Giannoulis, K., et al., *Serum concentrations of soluble ICAM-1 and VCAM-1 in patients with colorectal cancer. Clinical implications*. Tech Coloproctol, 2004. **8 Suppl 1**: p. s65-7.
42. Maurer, C.A., et al., *Over-expression of ICAM-1, VCAM-1 and ELAM-1 might influence tumor progression in colorectal cancer*. Int J Cancer, 1998. **79**(1): p. 76-81.
43. Hayes, S.H. and G.M. Seigel, *Immunoreactivity of ICAM-1 in human tumors, metastases and normal tissues*. Int J Clin Exp Pathol, 2009. **2**(6): p. 553-60.
44. Kostler, W.J., et al., *Soluble ICAM-1 in breast cancer: clinical significance and biological implications*. Cancer Immunol Immunother, 2001. **50**(9): p. 483-90.
45. Rosette, C., et al., *Role of ICAM1 in invasion of human breast cancer cells*. Carcinogenesis, 2005. **26**(5): p. 943-50.
46. Guo, P., et al., *ICAM-1 as a molecular target for triple negative breast cancer*. Proc Natl Acad Sci U S A, 2014. **111**(41): p. 14710-5.
47. Roland, C.L., et al., *ICAM-1 expression determines malignant potential of cancer*. Surgery, 2007. **141**(6): p. 705-7.
48. Tseng, P.H., et al., *Overcoming trastuzumab resistance in HER2-overexpressing breast cancer cells by using a novel celecoxib-*

- derived phosphoinositide-dependent kinase-1 inhibitor. Mol Pharmacol, 2006. 70(5): p. 1534-41.*
49. Levenson, A.S. and V.C. Jordan, *MCF-7: the first hormone-responsive breast cancer cell line. Cancer Res, 1997. 57(15): p. 3071-8.*
 50. Likhite, N. and U.M. Warawdekar, *A unique method for isolation and solubilization of proteins after extraction of RNA from tumor tissue using trizol. J Biomol Tech, 2011. 22(1): p. 37-44.*
 51. Desjardins, P. and D. Conklin, *NanoDrop microvolume quantitation of nucleic acids. J Vis Exp, 2010(45).*
 52. Liu, Z.Q., T. Mahmood, and P.C. Yang, *Western blot: technique, theory and trouble shooting. N Am J Med Sci, 2014. 6(3): p. 160.*
 53. Technologies, L. *Real time PCR handbook. [cited 2016 16 May]; Available from: <http://www.gene-quantification.com/real-time-pcr-handbook-life-technologies-update-flr.pdf>.*
 54. Hutchins, D. and C.M. Steel, *Regulation of ICAM-1 (CD54) expression in human breast cancer cell lines by interleukin 6 and fibroblast-derived factors. Int J Cancer, 1994. 58(1): p. 80-4.*
 55. Budinsky, A.C., et al., *Decreased expression of ICAM-1 and its induction by tumor necrosis factor on breast-cancer cells in vitro. Int J Cancer, 1997. 71(6): p. 1086-90.*
 56. Jahnke, A., et al., *Constitutive expression of human intercellular adhesion molecule-1 (ICAM-1) is regulated by differentially active enhancing and silencing elements. Eur J Biochem, 1995. 228(2): p. 439-46.*
 57. Caldenhoven, E., et al., *Stimulation of the human intercellular adhesion molecule-1 promoter by interleukin-6 and interferon-gamma involves binding of distinct factors to a palindromic response element. J Biol Chem, 1994. 269(33): p. 21146-54.*
 58. van de Stolpe, A., et al., *Glucocorticoid-mediated repression of intercellular adhesion molecule-1 expression in human monocytic and bronchial epithelial cell lines. Am J Respir Cell Mol Biol, 1993. 8(3): p. 340-7.*

59. Guo, P., et al., *ICAM-1-Targeted, Lcn2 siRNA-Encapsulating Liposomes are Potent Anti-angiogenic Agents for Triple Negative Breast Cancer*. *Theranostics*, 2016. **6**(1): p. 1-13.

7. Appendices

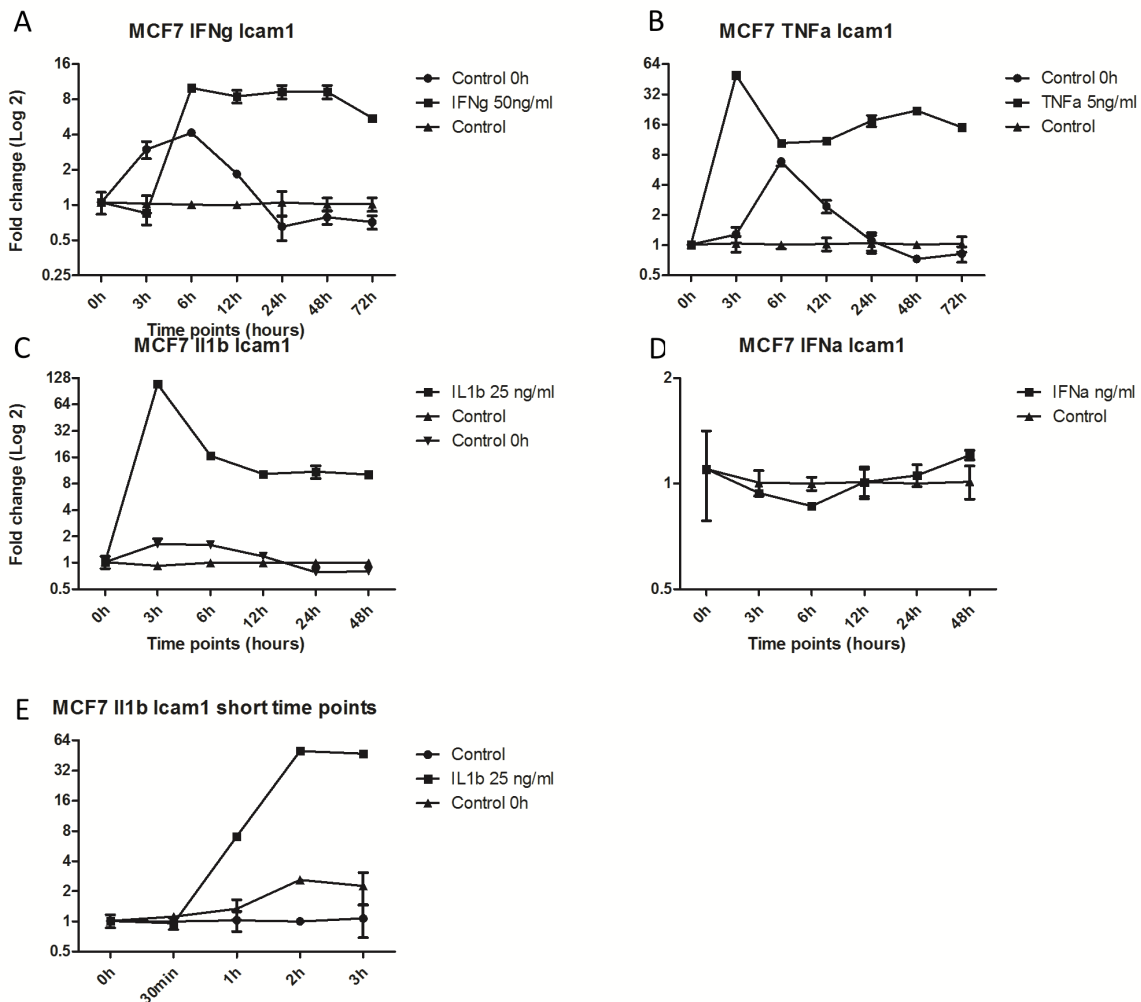


Figure A1, A-E: Gene expression of ICAM-1 in MCF7 cell lines stimulated with IFN γ (A), TNF α (B), IL-1 β at 3 to 48 hours (C), IFN α (D) and IL-1 β at 30 minutes to 3 hours. qPCR detecting ICAM-1 was performed on RNA isolated from cell lines stimulated with named cytokines. Expression levels of ICAM-1 were normalised against the expression level of TBP and RPLPO. Data is given as Log 2 of mean SEM of fold change values normalised against time-matched unstimulated control groups.

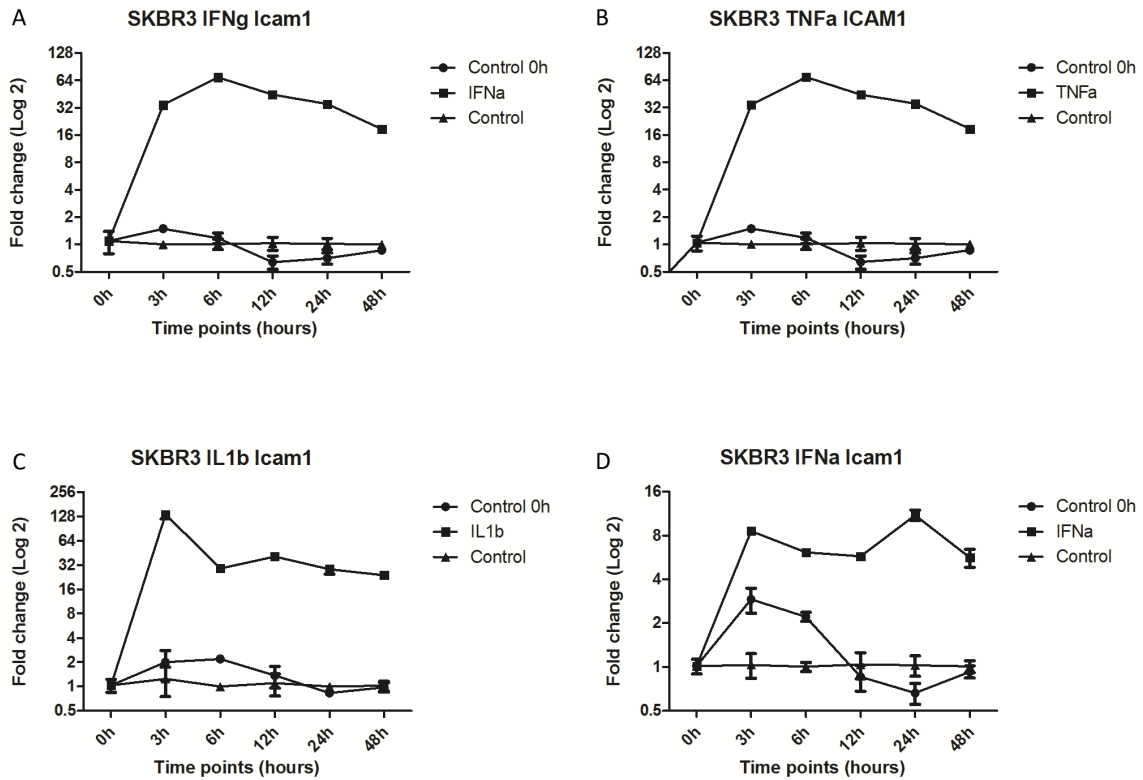


Figure A2, A-D: Gene expression of ICAM-1 in SK-BR-3 cell lines stimulated with IFN γ (A), TNF α (B), IL-1 β (C), and IFN α (D). qPCR detecting ICAM-1 was performed on RNA isolated from cell lines stimulated with named cytokines. Expression levels of ICAM-1 were normalised against the expression level of RPLPO. Data is given as Log 2 of mean SEM of fold change values normalised against time-matched unstimulated control groups.

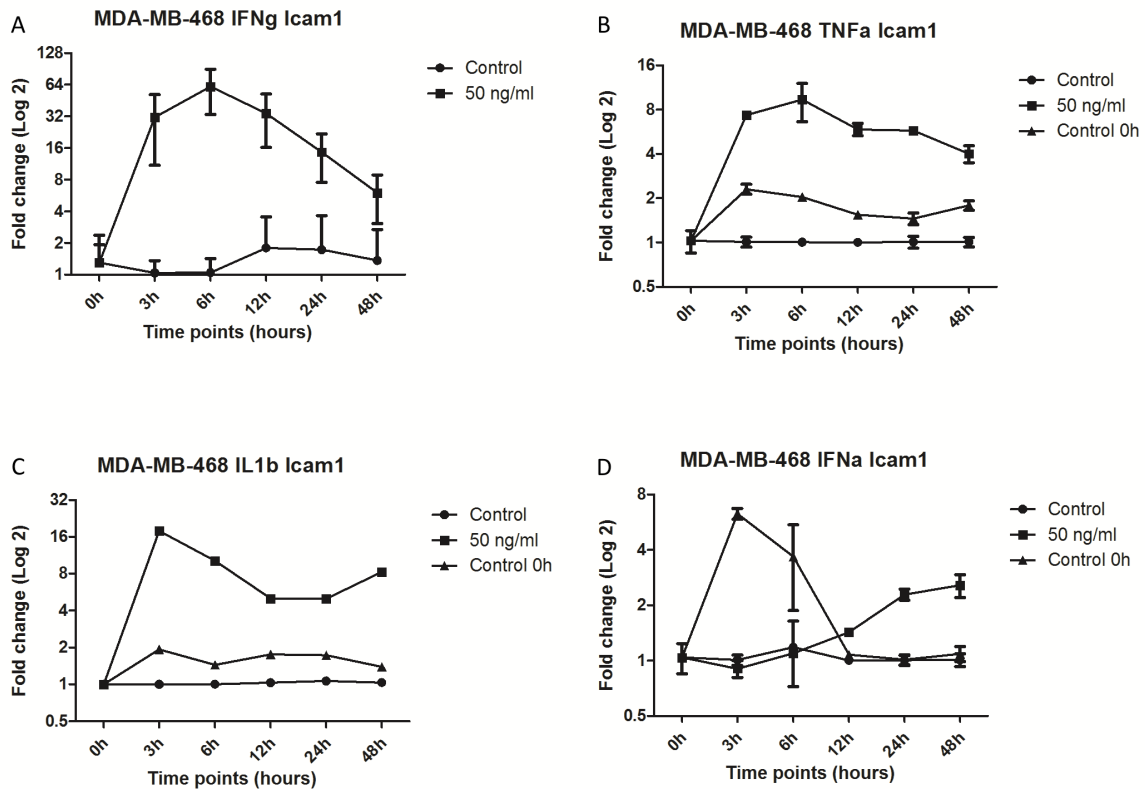


Figure A3, A-D: Gene expression of ICAM-1 in MDA-MB-468 cell lines stimulated with IFN γ (A), TNF α (B), IL-1 β (C), and IFN α (D). qPCR detecting ICAM-1 was performed on RNA isolated from cell lines stimulated with named cytokines. Expression levels of ICAM-1 were normalised against the expression level of RPLP0. Data is given as Log 2 of mean SEM of fold change values normalised against time-matched unstimulated control groups.

Table A1. Clinicopathological characteristics of human breast cancer cohort.

Lib #	ER (%)	PGR (%)	HER2	Tumor size mm.	pTNM-classification	LN metastasis	Tumour grade	Inflammatory aggregates
1	ND*	ND	ND	dcis	pTis (DCIS)	No	dcis	Neg
3	Neg ^{&}	Pos (>10)	Pos	30	pT2	No	3	Pos
4	Pos [£] (>90)	Pos (>70)	Neg	15	pT1c N1	Yes	1	Neg
6	Pos (>90)	Pos (>80)	Neg	60	pT3 N0(ITC)	Yes	2	Neg
7	Pos (>90)	Pos (>60)	Neg	25	pT2 N2a	Yes	2	Pos
9	Pos (>90)	Pos (>90)	Neg	20	pT1c N0	No	2	Pos
10	Pos (100)	Pos (100)	Neg	10	pT1b	No	2	Neg
11	Neg	Neg	Pos	16	pT1c N0 Mx	No	3	Pos
12	Pos (>90)	Pos (>60)	Neg	7	pT1b N0	No	2	Pos
13	Neg	Neg	Neg	19	pT1c N0(i+)	No	3	Pos
15	Pos (>80)	Pos (>80)	Neg	32	pT2 N0	No	2	Pos
16	Pos (>90)	Pos (>50)	Neg	25	pT2 N1a	Yes	2	Pos
17	Pos (>60)	Pos (>60)	Neg	12	pT1c	No	1	Neg
18	Pos (>90)	Pos (>90)	Neg	12	pT1 N0	No	1	Neg
20	Pos (>90)	Pos (>90)	Neg	20	pT1c N0	No	2	Pos
21	Pos (>90)	Pos (>30)	Neg	13	pT1c N0	No	1	Neg
22	Pos (>90)	Pos (>90)	Neg	28	pT2 N0	No	3	Pos
24	Pos (>90)	Pos (>90)	Neg	15	pT1c N0	No	1	Neg
25	Pos (>90)	Pos (>90)	Neg	13	pT1c N0	No	1	Pos
26	Pos (>90)	Pos (>90)	Neg	45	ND	No	1	Neg
27	Neg	Neg	Pos	30	pT2 N0	No	2	Pos
30	Pos (>95)	Pos (>80)	Neg	20	pT1c N1a	Yes	1	Neg
31	Pos (>95)	Pos (>90)	Neg	40	pT2 N0	No	1	Neg

*ND; not done, &Neg; negative, £Pos; positive,

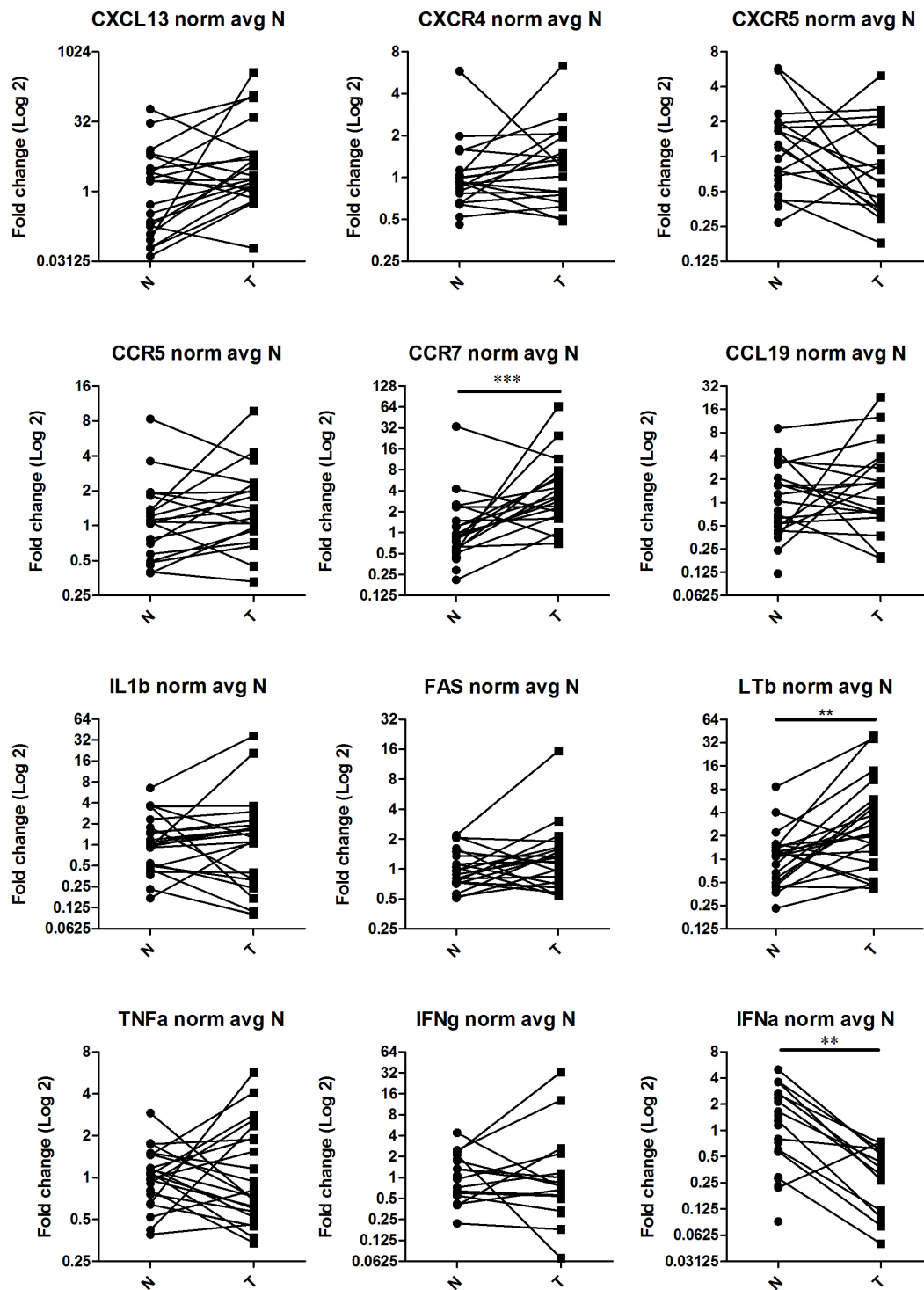


Figure A4. Gene expression in human tumour samples compared with the expression in matched normal tissue from the same patient normalised against the average gene expression of the normal tissue (N). Significant differences marked ***P<0.001, **P<0.01.

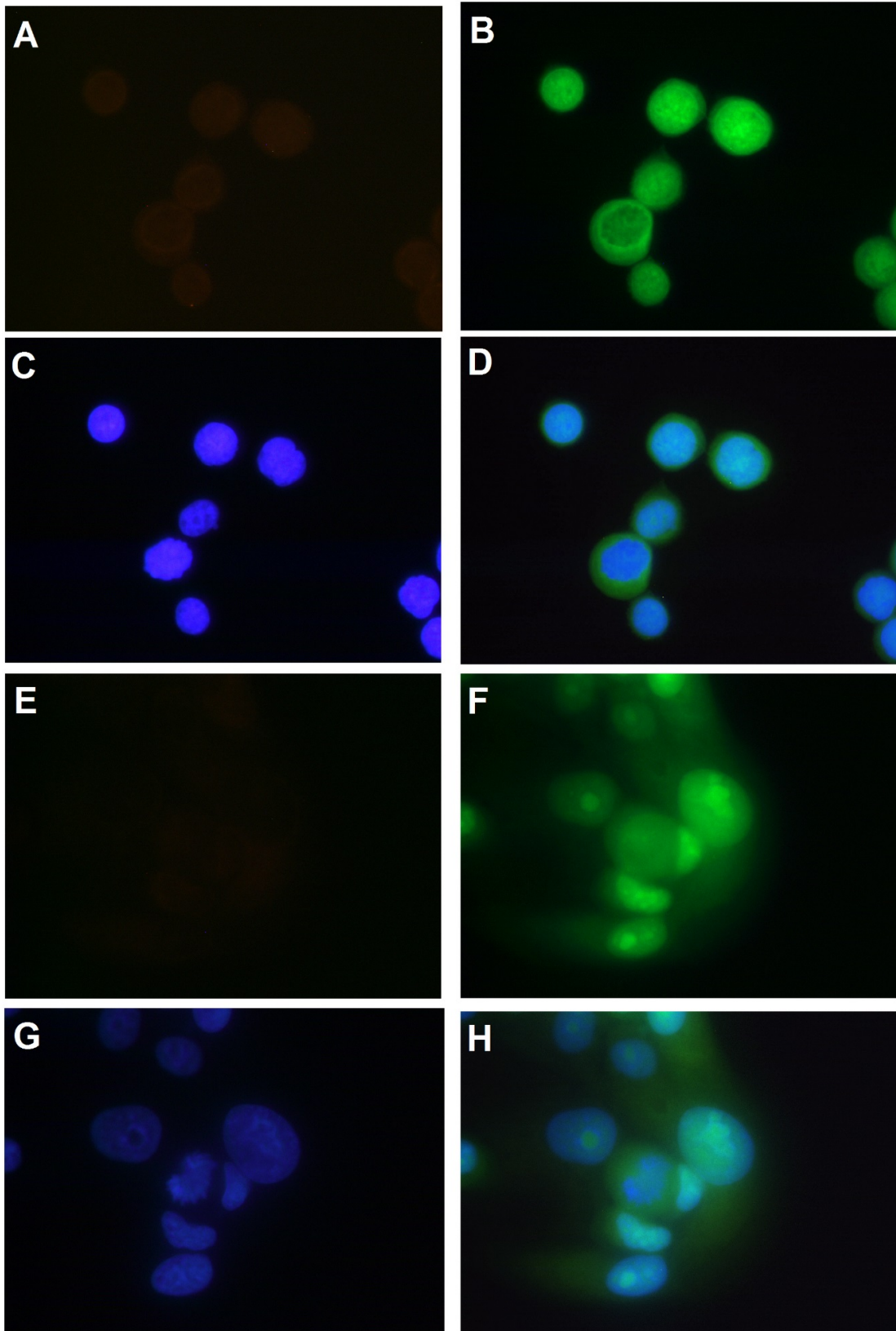


Figure A5. Immunofluorescence in MDA-MB-468(A-D) and MCF7 (E to H) cells where the primary antibody was omitted. A and E show Alexa Fluor 546 secondary antibody signal, B and F highlight cytoplasm with Cell Tracker Green™, C and H show nuclear staining with DAPI, D and H are composite images. High power magnification (600x).

Table A2. Spearman correlation matrix, human breast cancer specimens, correlation coefficients

	CXCL13	CXCR4	CXCR5	CCR5	CCR7	CCL19	ICAM1	LTBr	LTB	FAS	IL1B	T gr	LK met	ER	PGR	HER2	INF Gr
CXCL13		-0,00981	0,104798	0,050276	0,041667	0,002451	-0,1214	-0,48039	0,04902	-0,03679	-0,33865	-0,35436	-0,28988	0,191052	0,040996	0	-0,27741
CXCR4	-0,00981		0,462734	0,536436	0,618693	0,151821	0,121159	0,191396	0,265029	-0,18262	-0,02285	-0,13206	-0,26198	0,186765	0	-0,47703	-0,04355
CXCR5	0,104798	0,462734		0,62526	0,304191	0,450079	0,492755	0,104555	0,222453	0,117952	0,105645	-0,11872	-0,20374	-0,07898	-0,14953	-0,05607	0,123395
CCR5	0,050276	0,536436	0,62526		0,428258	0,382624	0,4741	0,14662	0,274682	0,095698	0,130932	-0,07962	0,130988	0,129366	-0,10227	-0,40909	0,080181
CCR7	0,041667	0,618693	0,304191	0,428258		0,621053	0,278192	0,19921	0,712281	-0,0351	-0,34168	-0,00339	0,071833	-0,06815	-0,37481	-0,05541	
CCL19	0,002451	0,151821	0,450079	0,382624	0,621053		0,600263	0,471259	0,471259	0,159789	0,414572	0,307823	-0,31873	0,193842	-0,12016	-0,02247	0,132948
ICAM1	-0,1214	0,121159	0,492755	0,4741	0,278192	0,600263		0,159789	0,176393	0,367428	0,263181	0,264263	0,098241	-0,10062	0	-0,13636	0,144523
LTBr	-0,48039	0,191396	0,104555	0,14662	0,19921	0,471259	0,159789		0,414572	0,687006	0,104862	0,057751	0,056321	-0,0601	0,112403	-0,13488	0,095389
LTB	0,04902	0,265029	0,222453	0,274682	0,712281	0,680702	0,176393	0,414572		0,307823	-0,31873	0,193842	-0,01609	-0,12016	-0,02247	-0,06742	0,132948
FAS	-0,03679	-0,18262	0,117952	0,095698	-0,0351	0,358929	0,367428	0,687006	0,307823		0,280385	0,104303	0,06437	-0,16027	0,022481	0	0,190157
IL1B	-0,33865	-0,02285	0,105645	0,130932	-0,34168	-0,15898	0,263181	0,104862	-0,31873	0,280385		0,174068	-0,05635	-0,04009	-0,04499	-0,13497	0,106324
T gr	-0,35436	-0,13206	-0,11872	-0,07962	-0,00339	0,284444	0,264263	0,057751	0,193842	0,104303	0,174068		0,060757	-0,59131	-0,46183	0,461826	0,742653
LK met	-0,28988	-0,26198	-0,20374	0,130988	-0,21822	0,152753	0,098241	0,056321	-0,01609	-0,06437	-0,05635	0,060757		0,024056	-0,05407	-0,24333	0,049152
ER	0,191052	0,186765	-0,07898	0,129366	0,071833	-0,10057	-0,10062	-0,0601	-0,12016	-0,16027	-0,04009	-0,59131	0,024056		0,842927	-0,84293	-0,28429
PGR	0,040996	0	-0,14953	-0,10227	-0,06815	0	0,112403	-0,02247	0,022481	-0,04499	-0,46183	-0,05407	0,842927	0,842927		-0,61404	-0,3081
HER2	0	-0,47703	-0,05607	-0,40909	-0,37481	-0,17037	-0,13636	-0,13488	-0,06742	0	-0,13497	0,461826	-0,24333	-0,84293	-0,61404		0,171169
INF Gr	-0,27741	-0,04355	0,123395	0,080181	-0,05541	0,259236	0,144523	0,095389	0,132948	0,190157	0,106324	0,742653	0,049152	-0,28429	-0,3081	0,171169	

Table A3. Spearman correlation matrix, human breast cancer specimens, P-values

	CXCL13	CXCR4	CXCR5	CCR5	CCR7	CCL19	ICAM1	LTBr	LTB	FAS	IL1B	T gr	LK met	ER	PGR	HER2	INF Gr
CXCL13		0,970192	0,699309	0,848037	0,873844	0,992551	0,642552	0,050962	0,851794	0,888525	0,18364	0,178097	0,259068	0,478457	0,880178	1	0,281039
CXCR4	0,970192		0,053152	0,017894	0,004743	0,534956	0,621241	0,432491	0,272833	0,454283	0,926032	0,601413	0,2786	0,458051	1	0,045316	0,859473
CXCR5	0,699309	0,053152		0,005522	0,219722	0,060905	0,037743	0,679696	0,374959	0,64112	0,676527	0,649966	0,417426	0,763164	0,566778	0,830738	0,625686
CCR5	0,848037	0,017894	0,005522		0,067355	0,105918	0,040294	0,549196	0,255083	0,696747	0,593147	0,753493	0,592986	0,608925	0,686347	0,091849	0,744199
CCR7	0,873844	0,004743	0,219722	0,067355		0,004541	0,248814	0,413568	0,000623	0,886554	0,152217	0,989361	0,369452	0,776987	0,788178	0,125398	0,821747
CCL19	0,992551	0,534956	0,060905	0,105918	0,004541		0,006582	0,041676	0,001337	0,131264	0,515633	0,252631	0,532423	0,691335	0,788178	0,499116	0,283843
ICAM1	0,642552	0,621241	0,037743	0,040294	0,248814	0,006582		0,513473	0,470063	0,121727	0,276315	0,289297	0,689067	0,691183	1	0,589515	0,554985
LTBr	0,050962	0,432491	0,679696	0,549196	0,413568	0,041676	0,513473		0,055066	0,000413	0,642348	0,80363	0,803402	0,795805	0,627607	0,559933	0,672832
LTB	0,851794	0,272833	0,374959	0,255083	0,000623	0,001337	0,470063	0,055066		0,163423	0,148246	0,399827	0,943354	0,603892	0,922972	0,771534	0,555318
FAS	0,888525	0,454283	0,64112	0,696747	0,886554	0,131264	0,121727	0,000413	0,163423		0,206269	0,652756	0,775966	0,487704	0,922947	1	0,396646
IL1B	0,18364	0,926032	0,676527	0,593147	0,152217	0,515633	0,276315	0,642348	0,148246	0,206269		0,450476	0,803293	0,863009	0,846454	0,559676	0,637688
T gr	0,178097	0,601413	0,649966	0,753493	0,989361	0,252631	0,289297	0,80363	0,399827	0,652756	0,450476		0,788247	0,003752	0,030485	0,030485	7,54E-05
LK met	0,259068	0,2786	0,417426	0,592986	0,369452	0,532423	0,689067	0,803402	0,943354	0,775966	0,803293	0,788247		0,915374	0,811107	0,275179	0,823757
ER	0,478457	0,458051	0,763164	0,608925	0,776987	0,691335	0,691183	0,795805	0,603892	0,487704	0,863009	0,003752	0,915374		8,48E-07	8,48E-07	0,19975
PGR	0,880178	1	0,566778	0,686347	0,788178	0,788178	1	0,627607	0,922972	0,922947	0,846454	0,030485	0,811107	8,48E-07		0,002366	0,163017
HER2	1	0,045316	0,830738	0,091849	0,125398	0,499116	0,589515	0,559933	0,771534	1	0,559676	0,030485	0,275179	8,48E-07	0,002366		0,446276
INF Gr	0,281039	0,859473	0,625686	0,744199	0,821747	0,283843	0,554985	0,672832	0,555318	0,396646	0,637688	7,54E-05	0,823757	0,19975	0,163017	0,446276	